1521-009X/47/3/340–349$35.00
DRUG METABOLISM AND DISPOSITION

https://doi.org/10.1124/dmd.118.084897
Drug Metab Dispos 47:340–349, March 2019



# Pharmacokinetics, Metabolism, and Excretion of [$^{14}$C]Esaxerenone, a Novel Mineralocorticoid Receptor Blocker in Humans[S]

Makiko Yamada, Jeanne Mendell, Hideo Takakusa, Takako Shimizu, and Osamu Ando

*Drug Metabolism and Pharmacokinetics Research Laboratories (M.Y., H.T., O.A.) and Clinical Pharmacology Department (T.S.), Daiichi Sankyo Co., Ltd., Tokyo, Japan; and Daiichi Sankyo Pharma Development, Basking Ridge, New Jersey (J.M.)*

Received October 15, 2018; accepted December 5, 2018

## ABSTRACT

**Esaxerenone (CS-3150) is a novel, nonsteroidal, selective mineralocorticoid receptor blocker. The absorption, metabolism, distribution, and excretion of esaxerenone were assessed in in vitro studies and in a clinical study, where [$^{14}$C]esaxerenone (150 $\mu$Ci/20 mg) was administered orally to six healthy male subjects. The plasma concentrations of esaxerenone and its metabolites (M4, M11, and M1) were measured using liquid chromatography–tandem mass spectrometry. The recovery of radioactivity was 92.5%, with 38.5% and 54.0% excreted in the urine and feces, respectively. The half-life of radioactivity in blood and plasma was approximately 30 hours, similar to that of the unchanged form in plasma. The blood-to-plasma ratio was 0.628, demonstrating low partitioning to blood components. In plasma, esaxerenone was the most abundant moiety (40.8%), followed by *O*-glucuronide (21.4%; M4), acyl-glucuronide of amide-bond hydrolysate (8.0%; M11), and the deshydroxyethyl form (1.7%; M1). In vitro studies showed that esaxerenone was a substrate of CYP3A and multiple UDP-glucuronosyltransferase isoforms. Oxidation contributed approximately 30% to its clearance, as indicated by the excretion ratio of oxidized metabolites into urine and feces. Caco-2 studies showed that esaxerenone was a substrate of P-glycoprotein and breast cancer resistance protein; however, the excretion ratios of the unchanged form in the feces and urine were 18.7% and 1.6%, respectively, indicating that these transporters were not important for the absorption and elimination of esaxerenone. Low urinary excretion of esaxerenone suggested that the plasma exposure of esaxerenone was not affected by renal dysfunction. Multiple elimination pathways including oxidation, glucuronidation, and hydrolysis, and the low contribution of transporters, indicated limited drug-drug interaction potential.**

## Introduction

Mineralocorticoid receptors (MRs) that are present in the epithelial cells of the distal tubule and collecting duct in the kidney have been reported to play a role in the regulation of electrolyte homeostasis, body fluids, and blood pressure via activation by aldosterone (Funder, 1995). In addition, MRs have been reported to be expressed in nonepithelial tissues such as podocytes (Shibata et al., 2007), mesangial cells (Nishiyama et al., 2005), fibroblasts (Nagai et al., 2005), and the heart (Lombès et al., 1995). Excessive MR activation by endogenous ligands (e.g., aldosterone) is involved in the pathogenesis of renal disorders, which may be caused by direct enhancement of fibrosis (Brem et al., 2011), inflammation (Siragy and Xue, 2008), and oxidative stress (Patni et al., 2007). Multiple clinical studies using steroidal MR blockers, such as spironolactone and eplerenone, have shown that MR blockade is a favorable strategy for the treatment of hypertension (Saruta et al., 2004), heart failure (Pitt et al., 1999, 2003), and chronic kidney disease (Rossing et al., 2005; Epstein et al., 2006). However, the clinical use of existing MR antagonists is limited by their safety and efficacy profiles (Rose et al., 1977; Weinberger et al., 2002).

Esaxerenone (CS-3150) is a novel, nonsteroidal, selective MR blocker. An in vitro study showed that esaxerenone inhibited the binding of aldosterone to the MR, with no agonistic or antagonistic effects on glucocorticoid, androgen, or progesterone receptors, even at high concentrations (Arai et al., 2015a). In pharmacology studies using rat models, esaxerenone was demonstrated to have potent and long-lasting antihypertensive and cardio-renal protective effects (Arai et al., 2015a, b, 2016). In clinical studies, esaxerenone dose dependently reduced blood pressure in patients with hypertension (submitted manuscript); furthermore, the reduction of urinary albumin in patients with type 2 diabetes with microalbuminuria underscores its renal protective effects (submitted manuscript). In pharmacokinetic studies, the absolute oral bioavailability of esaxerenone was high in rats and monkeys (Yamada et al., 2017). The elimination half-life at the terminal phase ($t_{1/2}$) of esaxerenone in plasma is longer than that of spironolactone and eplerenone in rats, and is considered to contribute to its long-lasting pharmacological effects. In rats, orally administered [$^{14}$C]esaxerenone was distributed widely to tissues, with the exception of a low distribution to the central nervous system (Yamada et al., 2017). After the oral administration of [$^{14}$C]esaxerenone, the major elimination pathway was oxidation in rats, and oxidation and glucuronidation in monkeys, and the radioactivity was excreted mainly in the feces (Yamada et al., 2017). In phase 1 studies, the

https://doi.org/10.1124/dmd.118.084897.
[S]This article has supplemental material available at dmd.aspetjournals.org.

**ABBREVIATIONS:** ADME, absorption, distribution, metabolism, and excretion; AUC, area under the curve; AUCR, area under the curve ratio; BCRP, breast cancer resistance protein; DDI, drug-drug interaction; $F_a$, absorption ratio; HBSS, Hanks' balanced salt solution; LC-MS/MS, liquid chromatography–tandem mass spectrometry; LSC, liquid scintillation counter; MR, mineralocorticoid receptor; MS, mass spectrometry; 4MSA, 4-(methylsulfonyl)aniline; *m/z*, mass-to-charge ratio; $P_{app}$, permeability coefficient; P450, cytochrome P450; P-gp, P-glycoprotein; $t_{1/2}$, elimination half-life at the terminal phase; $T_{max}$, time to reach the maximum plasma concentration; UGT, UDP-glucuronosyltransferase.

exposure of esaxerenone after single (5–200 mg/d) and multiple (10–100 mg/d) doses was generally proportional to the dose (Kato et al., 2018). The times to reach the maximum plasma concentration ($T_{max}$) and $t_{1/2}$ after single oral administration were approximately 3 and 20 hours, respectively, and did not change across dose levels (Kato et al., 2018). The $t_{1/2}$ appears to be suitable for once-daily dosing because efficacy is expected to be sustained throughout the day. The total apparent clearance of drug and apparent volume of distribution also remained constant, regardless of dose. The exposure to esaxerenone in the multiple-dose treatment was greater on day 10 than on day 1, and the accumulation ratio was in the range of 1.36–1.98 (Kato et al., 2018).

Absorption, distribution, metabolism, and excretion (ADME) studies are an essential part of drug development since the ADME properties of a drug candidate are associated with its efficacy and safety. The use of radioactive tracers in ADME studies, such as $^{14}$C-labeled compounds, enables us to determine the major metabolic and excretory routes of elimination of a drug candidate. Such information is necessary to determine the drug-drug interaction (DDI) potential and the influence of renal or hepatic dysfunction. The guidance on metabolites in safety testing from the Food and Drug Administration states that the exposure of metabolites should be determined to evaluate the necessity of additional safety assessment of metabolites (Food and Drug Administration, 2016). Owing to the evolution of analytical techniques, in most cases, metabolites in plasma can be detected without using labeled compounds. However, to prove that no metabolite that requires evaluation has been overlooked, studies using radiolabeled compounds are still necessary. In this study, [$^{14}$C]esaxerenone was administered to healthy male subjects and the pharmacokinetics, metabolism, and excretion were evaluated. In addition, the enzymes involved in the metabolism, cytochrome P450 (P450) and UDP-glucuronosyltransferase (UGT), and the transporters involved in the absorption of esaxerenone, P-glycoprotein (P-gp) and breast cancer resistance protein (BCRP), were evaluated.

## Materials and Methods

**Compounds and Reagents.** [$^{14}$C]esaxerenone [(5*P*)-1-(2-hydroxyethyl)-*N*-[4-(methanesulfonyl)phenyl]-4-methyl-5-[2-(trifluoromethyl)phenyl]-[4-$^{14}$C]-1*H*-pyrrole-3-carboxamide] was supplied by ABC Laboratories Inc. (Columbia, MO); the structure is shown in Fig. 1. Nonradiolabeled esaxerenone [(*S*)-1-(2-hydroxyethyl)-4-methyl-*N*-[4-(methylsulfonyl) phenyl]-5-[2-(trifluoromethyl) phenyl]-1*H*-pyrrole-3-carboxamide] and deuterium-labeled esaxerenone (Fig. 1) were synthesized at Daiichi Sankyo Co., Ltd. (Tokyo, Japan). The metabolites of esaxerenone, 4-methyl-*N*-[4-(methylsulfonyl)phenyl]-5-[2-(trifluoromethyl)-phenyl]-1*H*-pyrrole-3-carboxamide (M1), (*S*)-(3-methyl-4-{[4-(methylsulfonyl)-phenyl]carbamoyl}-2-[2-(trifluoromethyl)phenyl]-1*H*-pyrrol-1-yl)acetic acid (M2), (*S*)-1-(2-hydroxyethyl)-4-(hydroxymethyl)-*N*-[4-(methylsulfonyl)-phenyl]-5-[2-(trifluoromethyl)phenyl]-1*H*-pyrrole-3-carboxamide (M3), 2-[(*S*)-(3-methyl-4-{[4-(methylsulfonyl)phenyl]carbamoyl}-2-[2-(trifluoromethyl)-phenyl]-1*H*-pyrrol-1-yl)]ethyl β-D-glucopyranosiduronic acid (M4), ((*S*)-3-(hydroxymethyl)-4-{[4-(methylsulfonyl)phenyl]carbamoyl}-2-[2-(trifluoromethyl)-phenyl]-1*H*-pyrrol-1-yl)acetic acid (M5), and deuterium-labeled M1 were also synthesized at Daiichi Sankyo Co., Ltd. The metabolite M11, 1-*O*-({(5*P*)-1-(2-hydroxyethyl)-4-methyl-5-[2-(trifluoromethyl)phenyl]-1*H*-pyrrol-3-yl}carbonyl)-β-D-glucopyranuronic acid was synthesized at Daiichi Sankyo RD Novare (Tokyo, Japan). [$^{14}$C]4-(methylsulfonyl) aniline, a metabolite generated by the hydrolysis of esaxerenone, was synthesized at Curachem, Inc. (Chungcheongbuk, Korea). Esaxerenone and M1 were synthesized by using the method described in the patent applications (Canne Bannen et al., 2006; Aoki et al., 2008). M2 and M3 were prepared in a similar manner as that mentioned in the patent applications described previously. M4 was synthesized via conventional *O*-glycosidation of the alcohol in esaxerenone, followed by the removal of the protective group. M11 was prepared biosynthetically by using microorganisms from 1-(2-hydroxyethyl)-4-methyl-5-[2-(trifluoromethyl)phenyl]-1*H*-pyrrole-3-carboxylic acid.

Microsomes from baculovirus-infected insect cells expressing human P450 or UGT isoforms were purchased from BD Biosciences (San Jose, CA) and Corning Inc. (Corning, NY). A Reaction Phenotyping Kit (version 8) containing human liver microsomes from 16 individual donors was purchased from XenoTech, LLC (Kansas City, KS). NADPH regeneration system solution A, NADPH regeneration system solution B, UGT reaction mix solution A, and UGT reaction mix solution B were purchased from Corning Inc. Caco-2 cells were obtained from American Type Culture Collection (Manassas, VA). [$^{3}$H]Digoxin, [$^{3}$H]estrone sulfate ammonium salt, and [$^{14}$C]mannitol were purchased from PerkinElmer (Waltham, MA). [$^{14}$C]Theophylline was purchased from American Radiolabeled Chemicals (St. Louis, MO). Verapamil hydrochloride and novobiocin sodium salt were purchased from Sigma-Aldrich (St. Louis, MO). GF120918 was purchased from Toronto Research Chemicals (North York, Canada). Antibiotic-antimycotic (100×) liquid, L-glutamine-200 mM liquid, Dulbecco's modified Eagle's medium, fetal bovine serum, and 10× Hanks' balanced salt solution (HBSS) were purchased from Thermo Fisher Scientific (Waltham, MA). Other reagents were commercially available and of special reagent grade, high-performance liquid chromatography grade, liquid chromatography mass spectrometry (MS) grade, or equivalent.

**Clinical Study Design and Sample Collection.** The study was conducted at Worldwide Clinical Trials (San Antonio, TX) in six healthy male subjects between 18 and 60 years of age. The study was conducted in compliance with ethical principles that have their origin in the Declaration of Helsinki and was approved by the institutional review board (IntegReview, Austin, TX) on August 26, 2015. All participants provided written informed consent prior to commencement of the study. Each of the six subjects received a single oral dose of [$^{14}$C]esaxerenone (150 μCi/20 mg) as a solution after fasting for at least 8 hours. Subjects continued to fast for an additional 4 hours after dosing. Whole blood and plasma samples were collected at the following times: 0 (predose), 0.5, 1, 1.5, 2, 2.5, 3, 3.5, 4, 6, 8, 12, 16, 24, 36, 48, 60, 72, 96, 120, 132, 144, 156, 168, 180, 192, 216, 240, 264, and 288 hours postdose. Urine samples were collected over the following intervals: −2 to 0 hours (predose), 0–4, 4–8, 8–12, 12–24, 24–36, 36–48, 48–72, 72–96, 96–120, 120–144, 144–168, 168–192, 192–216, 216–240,

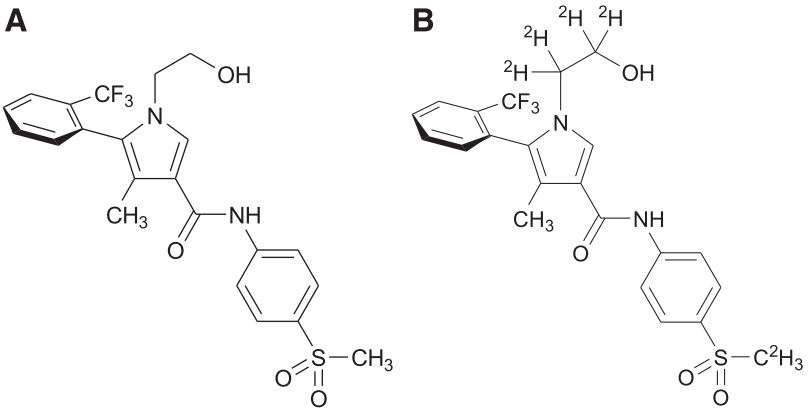


**Fig. 1.** Chemical structures of [$^{14}$C]esaxerenone (A) and deuterium-labeled esaxerenone (B).

240–264, and 264–288 hours postdose. The fecal samples were collected at the following times: 0, 0–24, 24–48, 48–72, 72–96, 96–120, 120–144, 144–168, 168–192, 192–216, 216–240, 240–264, and 264–288 hours postdose, and then mixed with water and homogenized. The samples were stored at approximately −80°C until analysis.

**Analysis of Total Radioactivity, Esaxerenone, and Metabolite Concentration.** The total radioactivity in blood, plasma, urine, and feces was measured by using a liquid scintillation counter (LSC) at Worldwide Clinical Trials. Plasma esaxerenone and metabolite concentrations were measured by a validated liquid chromatography–tandem mass spectrometry (LC-MS/MS) assay at Celerion (Lincoln, NE) using an electrospray ionization interface in the positive ion mode. The detailed method of analysis is shown in the Supplemental Material.

**Pharmacokinetic Analysis.** Plasma concentration-time data for esaxerenone and metabolites, and total radioactivity concentration-time data for [$^{14}$C]-esaxerenone equivalents in plasma and whole blood were analyzed by using noncompartmental methods in Phoenix WinNonlin (version 6.3; Pharsight Corporation, Mountain View, CA). The following parameters were calculated: the area under the curve (AUC) for the plasma concentration versus time up to the last measurable time point ($AUC_{last}$), area under the plasma concentration versus time curve to infinity ($AUC_{inf}$), maximum plasma concentration ($C_{max}$), $T_{max}$, and $t_{1/2}$. For esaxerenone, the apparent total body clearance and apparent volume of distribution based on the terminal phase were also calculated. The $AUC_{inf}$ and $t_{1/2}$ values were not calculated unless at least three time points (of which the first time point must be greater than $T_{max}$) with quantifiable concentrations were obtained. The blood-to-plasma $AUC_{last}$ ratio was calculated by dividing $AUC_{last}$ of total radioactivity in blood by $AUC_{last}$ of total radioactivity in plasma. The AUC ratio (AUCR) of esaxerenone and metabolites to total radioactivity (percentage) was calculated by dividing $AUC_{inf}$ of esaxerenone or metabolite by $AUC_{inf}$ of total radioactivity. $AUC_{last}$ was used for M1 instead of $AUC_{inf}$ because $AUC_{inf}$ was not calculated for M1. When calculating the AUCR, the AUC was converted into the molar amounts using the molecular weights of 466.47 for esaxerenone, 422.42 for M1, 642.60 for M4, and 489.40 for M11; the AUC for total radioactivity in molar amounts was determined by using the specific activity of [$^{14}$C]esaxerenone. The excretion of radioactivity in urine and feces (percentage of dose) was calculated by dividing excreted radioactivity by administered radioactivity.

**Metabolite Profiling of Human Plasma, Urine, and Feces.** The plasma samples collected at 1 hour postdose were pooled by mixing an equal volume from each subject, and qualitatively analyzed. The pooled urine (0–24 hours for qualitative analysis; 0–24, 24–48, and 48–72 hours for quantitative analysis) and feces (24–48 hours for qualitative analysis; 0–24, 24–48, 48–72, 72–96, and 96–168 hours for quantitative analysis) samples were prepared by proportional mixing from each subject based on the amount and combining a proportionally excreted amount from each time point, which were then used for analysis. The plasma, urine, or fecal samples were extracted with acetonitrile and analyzed by using a radio/high-performance liquid chromatography and MS detector, qualitatively and quantitatively. The detailed analysis method is shown in the Supplemental Material. For the quantitative analysis, the percentage area of each radioactive peak on the radiochromatogram was calculated with analysis software (FLO-ONE; PerkinElmer). The excretion ratios of esaxerenone and metabolites in urine and feces were calculated by multiplying the total excretion ratios of radioactivity in the urine and feces (percentage of dose) by the composition ratio of each radioactive peak, and shown as a cumulative value.

**In Vitro Identification of P450 Isoforms.** Two studies were conducted to identify the P450 isoforms involved in the oxidative metabolism of esaxerenone. For the recombinant study, esaxerenone was incubated with the microsomes from baculovirus-infected insect cells expressing human cytochrome P450 isoforms (CYP1A2, CYP2B6, CYP2C8, CYP2C9, CYP2C19, CYP2D6, CYP3A4, and CYP3A5; final concentration: 30 pmol P450/ml). For the correlation analysis, esaxerenone was incubated with each individual type of human liver microsomes (final concentration: 1 mg protein/ml). The concentrations of M1, M2, and M3 were measured by using the LC-MS/MS method. The detailed method is shown in the Supplemental Material. The formation rates of the metabolites were calculated by dividing the concentration of the metabolites by the incubation time and the P450 (nanomole P450 per milliliter) or protein (milligram protein per milliliter) concentration in microsomes. For the correlation analysis, the coefficient of determination ($R^2$) was calculated from the plot of each P450 isoform activity based on the specific marker reactions in individual human liver microsomes and the formation rates of the metabolites. The P450 isoform activities based on the specific marker reactions in individual human liver microsomes were cited from the data sheet provided by XenoTech, LLC.

**In Vitro UGT Isoform Identification.** Esaxerenone was incubated with the microsomes from baculovirus-infected insect cells expressing human UDP-glucuronosyltransferase isoforms (UGT1A1, UGT1A3, UGT1A4, UGT1A6, UTG1A9, UGT2B7, and UGT2B15; final concentration: 0.5 mg protein/ml), and the concentrations of M4 were measured by using the LC-MS/MS method. The detailed method is shown in the Supplemental Material. The formation rates of M4 were calculated by dividing the concentration of M4 by the incubation time and the protein concentration of the microsomes (milligram protein per milliliter).

**Transcellular Transport across Caco-2 Cells via P-gp and BCRP.** To evaluate the transcellular transport via P-gp and BCRP, Caco-2 cells were seeded at a density of $1 \times 10^5$ cells/cm$^2$ in 24-well plates. For the bidirectional transport assay, the medium at the apical and basal sides of the plate was removed by aspiration and replaced with HBSS or HBSS containing 100 $\mu$M verapamil (typical P-gp inhibitor) (Rautio et al., 2006), 10 $\mu$M novobiocin (typical BCRP inhibitor) (Xia et al., 2005), or 10 $\mu$M GF120918 (P-gp and BCRP inhibitor) (Xia et al., 2005), and the plate was preincubated at 37°C for 1 hour. After the preincubation, the solution in the donor side was replaced with HBSS buffer containing 1 $\mu$M [$^{14}$C]esaxerenone (with or without inhibitors), 1 $\mu$M [$^3$H]digoxin (typical P-gp substrate, with or without inhibitors), 0.1 $\mu$M [$^3$H]estrone sulfate (typical BCRP substrate, with or without inhibitors), 10 $\mu$M [$^{14}$C]theophylline (high-permeability marker), or 10 $\mu$M [$^{14}$C]mannitol (low-permeability marker). After incubation for a designated period at 37°C, the receiver side solution was collected into a glass vial. The assay solution (10 $\mu$l) was collected from the donor side after 1 hour and the radioactivity was counted by using the LSC. Incubation was performed in triplicate. The detailed method is shown in the Supplemental Material.

The permeability coefficient ($P_{app}$) and the $P_{app}$ ratio of the test compounds were calculated using the following equations:

$$P_{app}(\mathrm{cm/sec}) = [dQ/dt]/A/C_{donor}$$

where $dQ/dt$ is the transport rate (disintegrations per minute per second); $A$ is the surface area of the monolayer (square centimeters); and $C_{donor}$ is the observed concentration in donor sample collected after incubation for 1 hour (disintegrations per minute per milliliter).

$$P_{app}\mathrm{ratio} = P_{app,A\ to\ B}/P_{app,B\ to\ A}$$

where $P_{app,A\ to\ B}$ is the $P_{app}$ value from the apical-to-basal direction and $P_{app,B\ to\ A}$ is the $P_{app}$ value from the basal-to-apical direction.

**Metabolism and Excretion of Esaxerenone Hydrolysate in Rats.** In the course of the metabolite profiling, the hydrolysis of the central amide bond of esaxerenone was observed. Only the methyl-(trifluoromethyl)phenyl-hydroxyethyl-pyrrole carboxylate side was radiolabeled and detected; however, the complementary part, 4-(methylsulfonyl)aniline (4MSA), must also be produced in the body. Since the hydrolyzed metabolite was not observed in rats and monkeys, further nonclinical evaluation was difficult, even if another [$^{14}$C]esaxerenone with labeled 4MSA was synthesized. Therefore, [$^{14}$C]4MSA was synthesized to investigate its fate and administered intravenously to fasted male F344 rats (Charles River Laboratories Japan, Shiga, Japan) at 1 mg/kg. All animal experiments were conducted in accordance with the guidelines of the Institutional Animal Care and Use Committee of Daiichi Sankyo Co., Ltd. For the pharmacokinetic study ($n = 3$), the blood was collected from the jugular vein at the designated sample collection times and the plasma was obtained by centrifugation. The concentration of radioactivity in blood and plasma was measured by the LSC. For the mass balance study ($n = 3$), the rats were housed individually in the glass metabolic cages (Metabolica; Sugiyama-Gen Iriki, Tokyo, Japan) after the drug administration, and the urine and feces were collected for the designated periods. The concentration of radioactivity in the urine and feces was measured by the LSC and the excretion ratio of radioactivity (percentage of dose) was calculated by dividing the excreted radioactivity by the administered radioactivity. For metabolite profiling, the blood was collected from the abdominal aorta at 1 and 6 hours after administration and the plasma was obtained by centrifugation. The structure of metabolites was elucidated using LC-MS/MS coupled with a radioactivity detector. The detailed conditions of the analysis are shown in Supplemental Fig. 3.

## Results

### Pharmacokinetics and Excretion of [$^{14}$C]Esaxerenone

The radioactivity concentration-time profiles in blood and plasma after a single oral administration of 20 mg [$^{14}$C]esaxerenone to healthy volunteers are shown in Fig. 2A, and the pharmacokinetic parameters for radioactivity are shown in Tables 1. In plasma and blood, the mean $C_{max}$ values of radioactivity in plasma and blood were 430 and 281 ng-Eq/ml, the mean $AUC_{last}$ values were 12,600 and 7880 ng-Eq·h/ml, and the mean $AUC_{inf}$ values were 12,900 and 8180 ng-Eq·h/ml, respectively. The median $T_{max}$ and mean $t_{1/2}$ were approximately 4 and 30 hours both in blood and plasma, respectively. The blood-to-plasma $AUC_{last}$ ratio of the radioactivity was 0.628. Mean plasma concentrations of esaxerenone and its metabolites are shown in Fig. 2B. The pharmacokinetic parameters of esaxerenone and metabolites are presented in Tables 2. The mean $t_{1/2}$ of esaxerenone, M4, and M11 were 34.0, 27.8, and 26.4 hours, respectively. The $t_{1/2}$ times of M1 was not determined owing to its slow elimination; however, the exposure was very low. The mean $C_{max}$ value was 237 ng/ml for esaxerenone, followed by 165 ng/ml (for M4), 39.0 ng/ml (for M11), and 1.00 ng/ml (for M1). The mean exposure ($AUC_{last}$ for M1 and $AUC_{inf}$ for others) was 5320 ng·h/ml for esaxerenone, followed by 3860 ng·h/ml (for M4), 1070 ng·h/ml (for M11), and 198 ng·h/ml (for M1). Based on the $AUC_{inf}$ total radioactivity ratios, esaxerenone was the most abundant moiety in plasma (40.8%), followed by M4 (21.4%) and M11 (8.0%). Based on $AUC_{last}$, the abundance of M1 was 1.7% of the total radioactivity. The total recovery of radioactivity in urine and feces over the 288-hour sampling period was 92.5%, with 76.6% recovered by 96 hours and 86.7% recovered by 144 hours, as shown in Fig. 3. The cumulative percentages of radioactivity recovered in urine and feces were 38.5% and 54.0%, respectively.

### Structure Elucidation of Metabolites

Structural elucidation of the metabolites in plasma, urine, and feces collected after the oral administration of [$^{14}$C]esaxerenone was conducted by using LC-MS/MS combined with a radioactivity detector; representative radiochromatograms are shown in Fig. 4. Structural assignment and MS data are summarized in Table 3. The fragmentation schemes of esaxerenone and metabolites are shown in Supplemental Fig. 1.

**Plasma.** In plasma, unchanged esaxerenone was detected as the largest peak. Two radioactive peaks of the metabolites M4 and M11 were detected. M4 was identified to the *O*-glucuronide of esaxerenone, similar to that found in monkey plasma (Yamada et al., 2017). The structure of M4 is shown in Fig. 5. The deprotonated molecule $[M-H]^-$ ion of M11 was detected at mass-to-charge ratio (*m*/*z*) 488. One of the major product ions of M11 was detected at *m*/*z* 312, which corresponded to the loss of the glucuronic acid group (176 Da). The product ion at *m*/*z* 312 also corresponded to the methyl-(trifluoromethyl)-phenyl-hydroxyethyl-pyrrole carboxylate, suggesting that M11 was a glucuronide of the esaxerenone amide-bond hydrolysate. By comparing the retention time and LC-MS/MS spectra with those of the authentic standard, M11 was identified as the acyl-glucuronide of esaxerenone amide-bond hydrolysate; M1, which was identified in rat plasma (Yamada et al., 2017), was detected only by MS and was not detected by radiochromatography.

**Urine.** In urine, the unchanged form and metabolites (M2, M3, M4, M5, M8, M11, M12, and M13) were detected. M2, M3, and M5 were also detected in rat and monkey samples (Yamada et al., 2017), and identified as the carboxylic acid form in the *N*-alkyl side chain, the hydroxymethyl form of esaxerenone, and the hydroxymethyl form of M2 (or the carboxylic acid form of M3), respectively (Fig. 5).

The deprotonated molecule $[M-H]^-$ ion of M8 and M13 was detected at *m*/*z* 657, which was 192 Da larger than the *m*/*z* 465 of esaxerenone. The mass shift from esaxerenone corresponded to $C_6H_8O_7$, which was attributable to the combination of monooxygenation (+O) and glucuronidation ($+C_6H_8O_6$). In addition, the major fragment ions at *m*/*z* 481 and 463 were attributable to the loss of the glucuronic acid moiety and its dehydration product. Since the fragment ion at *m*/*z* 170 indicated no changes in the methylsulfonylphenyl group and the structure analysis of M3 demonstrated that the major oxidation site for esaxerenone was the methyl group on the pyrrole moiety as described subsequently, M8 and M13 were proposed to be glucuronides of M3; however, the conjugated position has not yet been determined.

The deprotonated molecule $[M-H]^-$ ion of M12 was detected at *m*/*z* 488. In the same way as M11, one of the major product ions at *m*/*z* 312 corresponded to the loss of the glucuronic acid group (176 Da) from the glucuronide of the esaxerenone amide-bond hydrolysate. Since M11

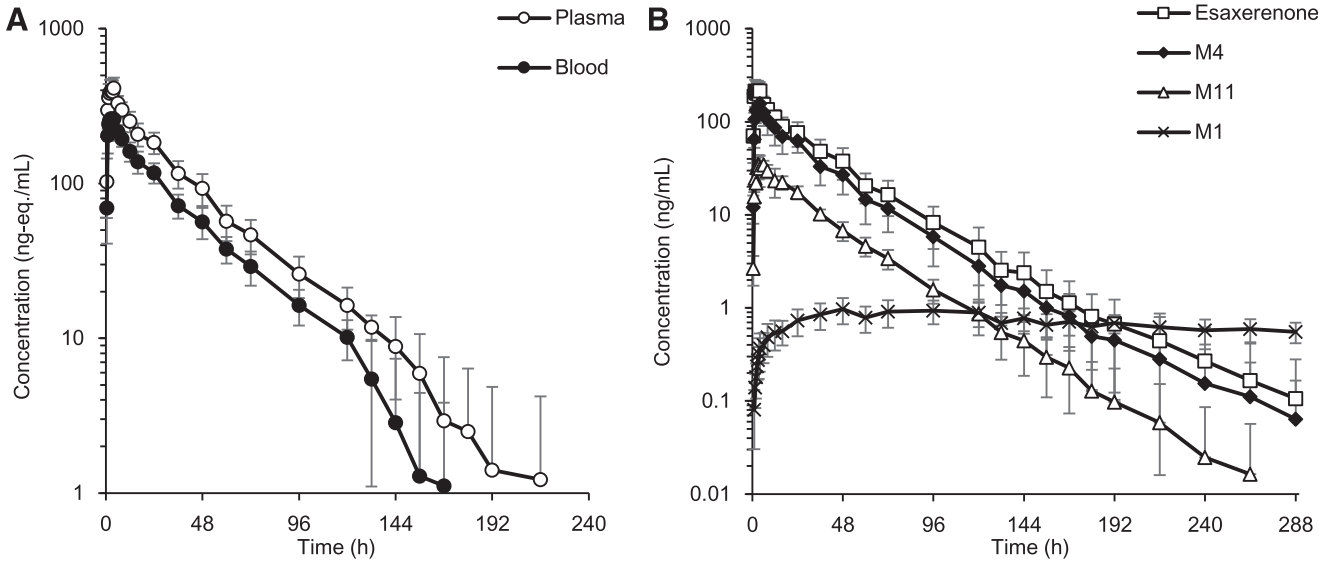


**Fig. 2.** Mean concentrations of radioactivity in blood and plasma (A) and esaxerenone and its metabolites M1, M4, and M11 in plasma (B) following a single oral administration of [$^{14}$C]esaxerenone. Each point represents the mean ± S.D. of six subjects.

TABLE 1

Pharmacokinetic parameters of radioactivity in blood and plasma

*Arithmetic means (S.D.) of six subjects, with the exception of $T_{max}$, for which the medians (minimum and maximum) are shown.*

| Parameter | Unit | $^{14}$C Plasma | $^{14}$C Blood |
|---|---|---|---|
| $C_{max}$ | ng-Eq/ml | 430 (65) | 281 (39) |
| $AUC_{last}$ | ng-Eq·h/ml | 12,600 (2100) | 7880 (1210) |
| $AUC_{inf}$ | ng-Eq·h/ml | 12,900 (2100) | 8180 (1240) |
| $t_{1/2}$ | h | 30.8 (3.9) | 29.6 (4.9) |
| $T_{max}$ | h | 3.75 (2.00, 6.02) | 3.25 (2.00, 6.02) |
| Blood-to-plasma $AUC_{last}$ ratio | 0.628 (0.014) | 0.628 (0.014) | 0.628 (0.014) |

was identified to be the acyl-glucuronide by using an authentic standard, M12 was estimated to be an *O*-glucuronide of esaxerenone amide-bond hydrolysate.

**Feces.** In feces, the unchanged form and metabolites (M2, M3, M5, M15, M16, and M17) were detected. The deprotonated molecule $[M-H]^-$ ion of M15 was detected at *m/z* 467, and its molecular composition was estimated to be $C_{21}H_{19}F_3N_2O_5S$ based on the accurate mass detected, which indicated that M15 was the demethylated ($-CH_2$) and monooxygenated (+O) form of esaxerenone. Together with mass fragmentation analysis, M15 was estimated as the sulfonic acid form of esaxerenone; assignment of the fragment ions is shown in Supplemental Fig. 1.

At the elution times of M16 and M17, *m/z* 497 was detected in the mass spectrum, and its accurate mass corresponded to $C_{22}H_{21}F_3N_2O_6S$, indicating that M16 and M17 were the dioxygenated (+2O) forms of esaxerenone. The site of oxidation for M16 was not identified because the product ion scan data were not obtained owing to the low intensity of the precursor ion. In the case of M17, the fragment ion *m/z* values of 170, 300, and 351 were detected as key fragment ions in the collision-induced dissociation and higher-energy C-trap dissociation product ion scan. From these data, the oxidation position for M17 was estimated to be on the pyrrole moiety containing the methyl and hydroxyethyl groups; assignment of the fragment ions is shown in Supplemental Fig. 1.

### Quantitative Metabolite Profiling

To assess the urinary and fecal excretion of the unchanged form and major metabolites, the urine collected from 0 to 72 hours and the feces collected from 0 to 168 hours were analyzed, and the results are shown in Table 4. After the oral administration of [$^{14}$C]esaxerenone to humans, the excretion of unchanged esaxerenone in urine was only 1.6%. M11 was excreted in urine at 10.5% of the dose as a major metabolite, followed by M4 (7.2%). In feces, esaxerenone was excreted at 18.7% of the dose and the major metabolites excreted were M3 and M5 (10.1%, sum of both metabolites) and M2 (9%). The total excretion ratio of the oxidized metabolites (M2, M3, M5, M16, and M17) and the conjugated forms of the oxidized metabolites (M8 and M13) was 28.9%.

### P450 and UGT Isoform Identification

Esaxerenone was incubated with microsomes from baculovirus-infected insect cells expressing human CYP1A2, CYP2B6, CYP2C8, CYP2C19, CYP2D6, CYP3A4, and CYP3A5, and the production of the oxidized metabolites (M1, M2, and M3) was determined by LC-MS/MS. The results are shown in Fig. 6A. The mean formation rates of M1, M2, and M3 in the microsomes expressing human P450 isoforms were 2.08, 2.06, and 136 pmol/min/nmol P450 for CYP3A4; and 0.647, 4.30, and 8.23 pmol/min/nmol P450 for CYP3A5, respectively. No metabolites were produced by other P450 isoforms. Esaxerenone was also incubated with human liver microsomes from 16 individual donors. The formation rates of metabolites by human liver microsomes were highly correlated with testosterone 6$\beta$-hydroxylation and midazolam 1′-hydroxylation, which are markers of CYP3A4/5 activity, with correlation coefficients ($r^2$) of 0.813, 0.842, and 0.807 for M1, M2, and M3, respectively (testosterone 6$\beta$-hydroxylation), and 0.707, 0.693, and 0.794, for M1, M2, and M3, respectively (midazolam 1′-hydroxylation). For the other P450 isoform activities, no apparent correlation was observed (Supplemental Fig. 2). These results indicated that CYP3A4 and CYP3A5 were the main isoforms involved in the oxidative metabolism of esaxerenone by P450 in the human liver. For UGT isoform identification, esaxerenone was incubated with microsomes from baculovirus-infected insect cells expressing human UGT1A1, UGT1A3, UGT1A4, UGT1A6, UTG1A9, UGT2B7, and UGT2B15; subsequently, the production of its metabolite, M4, was determined by LC-MS/MS. The results are shown in Fig. 6B. The formation rates of M4 for UGT1A1, UGT1A3, UGT1A4, UTG1A9, UGT2B7, and UGT2B15 were 0.932, 0.289, 0.115, 0.182, 0.837, and 0.668 pmol/min/nmol, respectively. These results indicated that multiple UGT isoforms were involved in the *O*-glucuronidation of esaxerenone.

TABLE 2

Pharmacokinetic parameters of esaxerenone and its metabolites in plasma after a single oral administration of [$^{14}$C]esaxerenone to healthy volunteers

*Arithmetic means (S.D.) of six subjects, with the exception of $T_{max}$, for which the medians (minimum and maximum) are shown.*

| Parameter | Unit | Esaxerenone | M4 | M11 | M1 |
|---|---|---|---|---|---|
| $C_{max}$ | ng/ml | 237 (60) | 165 (40) | 39.0 (2.9) | 1.00 (0.30) |
| $AUC_{last}$ | ng·h/ml | 5310 (1390) | 3860 (1190) | 1060 (70) | 198 (57) |
| $AUC_{inf}$ | ng·h/ml | 5320 (1390) | 3860 (1190) | 1070 (70) | NC |
| $t_{1/2}$ | h | 34.0 (9.8) | 27.8 (12.9) | 26.4 (10.2) | NC |
| $T_{max}$ | h | 2.25 (1.50, 4.00) | 4.00 (2.00, 6.02) | 3.75 (3.00, 6.02) | 48.0 (48.0, 96.0) |
| CL/F | l/h | 3.96 (0.94) | NC | NC | NC |
| $V_z$/F | l | 187 (36) | NC | NC | NC |
| AUCR[a] | % | 40.8 (5.7) | 21.4 (4.2) | 8.0 (0.8) | 1.7 (0.6) |

CL/F, apparent total body clearance; $V_z$/F, apparent volume of distribution based on the terminal phase; NC, not calculated.
[a]Metabolite/$^{14}$C plasma $AUC_{inf}$ ratio corrected for molecular weight; $AUC_{last}$ was used for M1.

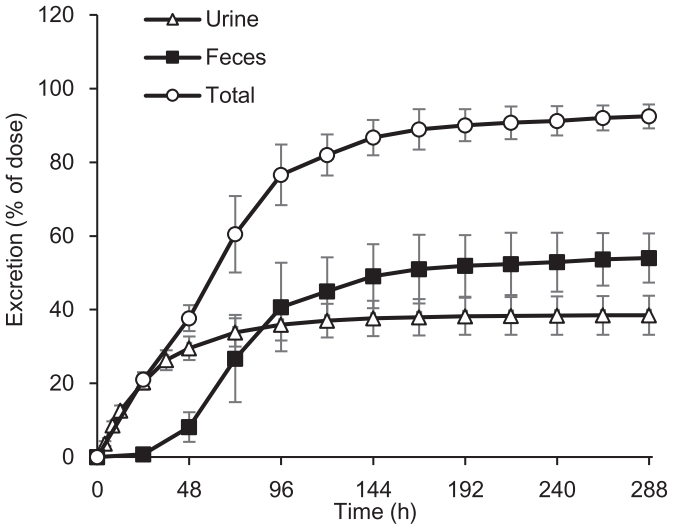


**Fig. 3.** Mean cumulative excretion of total radioactivity in urine and feces following a single oral administration of [$^{14}$C]esaxerenone. Each point represents the mean ± S.D. of six subjects.

### Transcellular Transport across Caco-2 Cell via P-gp and BCRP

The transcellular transport of [$^{14}$C]esaxerenone and the effects of P-gp and BCRP inhibitors investigated using Caco-2 cell monolayers are shown in Fig. 7. The electrical resistance was between 0.468 and 0.510 k$\Omega$•cm$^2$. The P-gp and BCRP activities in Caco-2 cell monolayers were confirmed by vectorial transport of [$^3$H]digoxin (a P-gp substrate) and [$^3$H]estrone sulfate (a BCRP substrate), which was inhibited in the presence of verapamil (a P-gp inhibitor) and novobiocin (a BCRP inhibitor), respectively (Fig. 7A). The vectorial transport of the two substrates was absent in the presence of GF120918 (an inhibitor of both P-gp and BCRP) as well (Fig. 7A). In the absence of the inhibitors, the apparent permeability coefficient ($P_{app}$) values for the apical-to-basal ($P_{app,A\ to\ B}$) and basal-to-apical directions ($P_{app,B\ to\ A}$) of [$^{14}$C]esaxerenone at 1 $\mu$M were $16.8 \times 10^{-6}$ and $43.5 \times 10^{-6}$ cm/s, respectively (Fig. 7B), and the $P_{app}$ ratio ($P_{app,B\ to\ A}/P_{app,A\ to\ B}$) was calculated as 2.59. Verapamil, novobiocin, and GF120918 affected the permeability of [$^{14}$C]esaxerenone (Fig. 7B). These results suggested that esaxerenone was a substrate of both P-gp and BCRP. The low $P_{app}$ of mannitol, a low-permeability marker drug, suggested the integrity of the Caco-2 cell monolayers during the study (Fig. 7B). Theophylline, of which 100% of the dose is absorbed in humans (Li et al., 2007), was evaluated as a highly membrane-permeable marker, and its $P_{app,A\ to\ B}$ was $22.4 \times 10^{-6}$ cm/s (Fig. 7B).

### Metabolism and Excretion of Esaxerenone Hydrolysate in Rats

$^{14}$C-Labeled 4-(methylsulfonyl)aniline ([$^{14}$C]4MSA), a metabolite generated by the hydrolysis of esaxerenone, was synthesized and administered to F344 rats to investigate the fate of the metabolite. After intravenous administration, the $t_{1/2}$ of the radioactivity in blood and plasma were 6.6 and 6.5 hours, respectively. By 24 hours after a single intravenous administration, 73.6% and 6.5% of the dosed radioactivity were excreted in urine and feces, respectively. By 96 hours after a single intravenous administration, 83.8% and 9.1% of the dosed radioactivity were excreted in the urine and feces, respectively, giving a total excretion of 92.9%. In the metabolite analysis of rat plasma, the acetylated form of 4MSA was mainly observed, and the hydroxylated

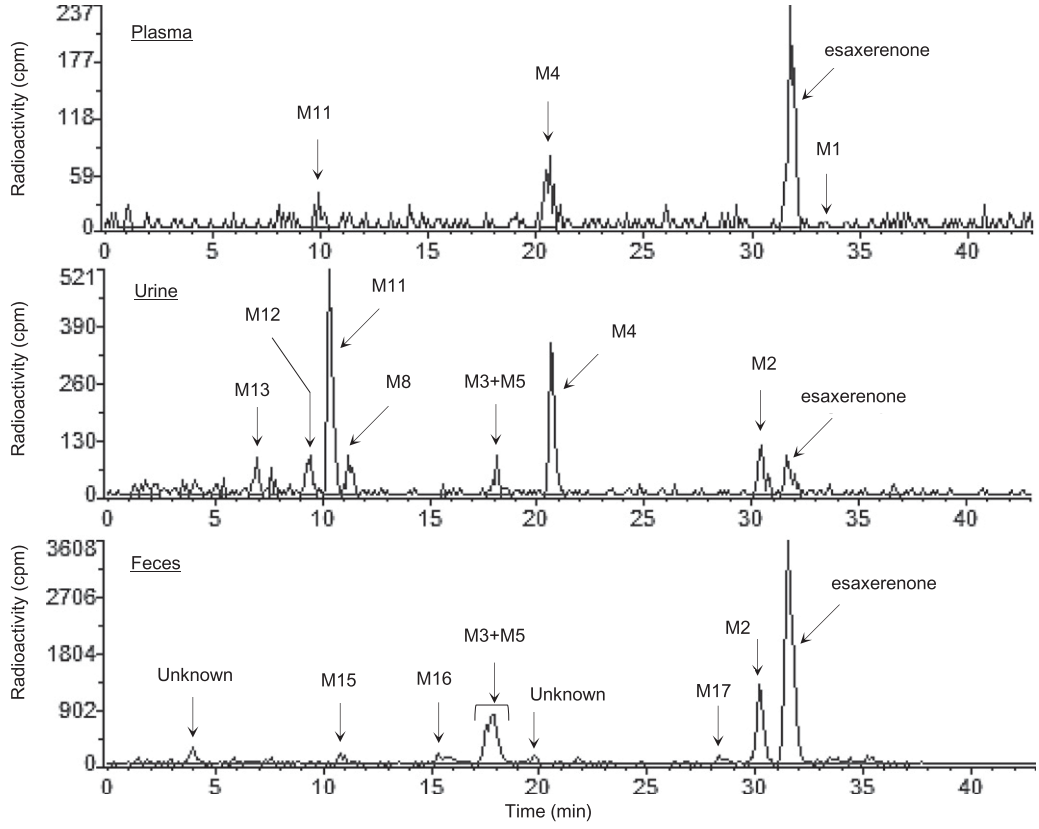


**Fig. 4.** Representative radiochromatograms of the metabolites in human plasma (1 hour), urine (0–24 hours), and feces (24–48 hours) following oral administration of [$^{14}$C]esaxerenone at a dose of 20 mg.

TABLE 3

Mass spectral analysis of esaxerenone metabolites detected in human plasma, urine, and feces

| Metabolite No. | Biotransformation | $[M-H]^-$ (*m/z*) | Elemental Composition | Characteristic Fragment Ions (*m/z*) |
|---|---|---|---|---|
| Esaxerenone | | 465 | $C_{22}H_{21}F_3N_2O_4S$ | 365, 224, 170 |
| M1 | Deshydroxyethyl form | 421 | $C_{20}H_{17}F_3N_2O_3S$ | 224, 184, 170 |
| M2 | Carboxylic acid form | 479 | $C_{22}CH_{19}F_3N_2O_5S$ | 365, 170 |
| M3 | Oxygenation | 481 | $C_{22}CH_{21}F_3N_2O_5S$ | 419, 381, 363, 351, 170 |
| M4 | *O*-glucuronide | 641 | $C_{28}H_{29}F_3N_2O_{10}S$ | 465, 447, 365, 224, 170 |
| M5 | Hydroxymethyl-carboxylic acid form | 495 | $C_{22}H_{19}F_3N_2O_6S$ | 381, 363, 351, 196, 170 |
| M8 | Glucuronide of monooxygenated form | 657 | $C_{28}H_{29}F_3N_2O_{11}S$ | 481, 419, 381, 170 |
| M11 | Acyl-glucuronide of amide-bond hydrolysate | 488 | $C_{21}H_{22}F_3NO_9$ | 312, 268, 238, 175 |
| M12 | *O*-glucuronide of amide-bond hydrolysate | 488 | $C_{21}H_{22}F_3NO_9$ | 312, 294, 268 |
| M13 | Glucuronide of monooxygenated form | 657 | $C_{28}H_{29}F_3N_2O_{11}S$ | 481, 419, 363, 170 |
| M15 | Sulfonic acid form | 467 | $C_{21}H_{19}F_3N_2O_5S$ | 343, 287, 198, 172 |
| M16 | Dioxygenated form | 497 | $C_{22}H_{21}F_3N_2O_6S$ | Not detected |
| M17 | Dioxygenated form | 497 | $C_{22}H_{21}F_3N_2O_6S$ | 351, 300, 170 |

form of the acetylated 4MSA was also identified. The detailed results are shown in Supplemental Fig. 3.

## Discussion

In this study, [$^{14}$C]esaxerenone was administered orally to six healthy male volunteers. The maximum dose of esaxerenone administered in a phase 3 study was 5 mg (https://clinicaltrials.gov/ct2/show/NCT02890173); however, 20 mg was administered in this study to ensure the feasibility of metabolite detection. The safety and dose proportionality after single doses of between 5 and 200 mg esaxerenone were confirmed in a phase 1 study (Kato et al., 2018); therefore, ADME profiles following administration of 20 mg were considered to be comparable with those

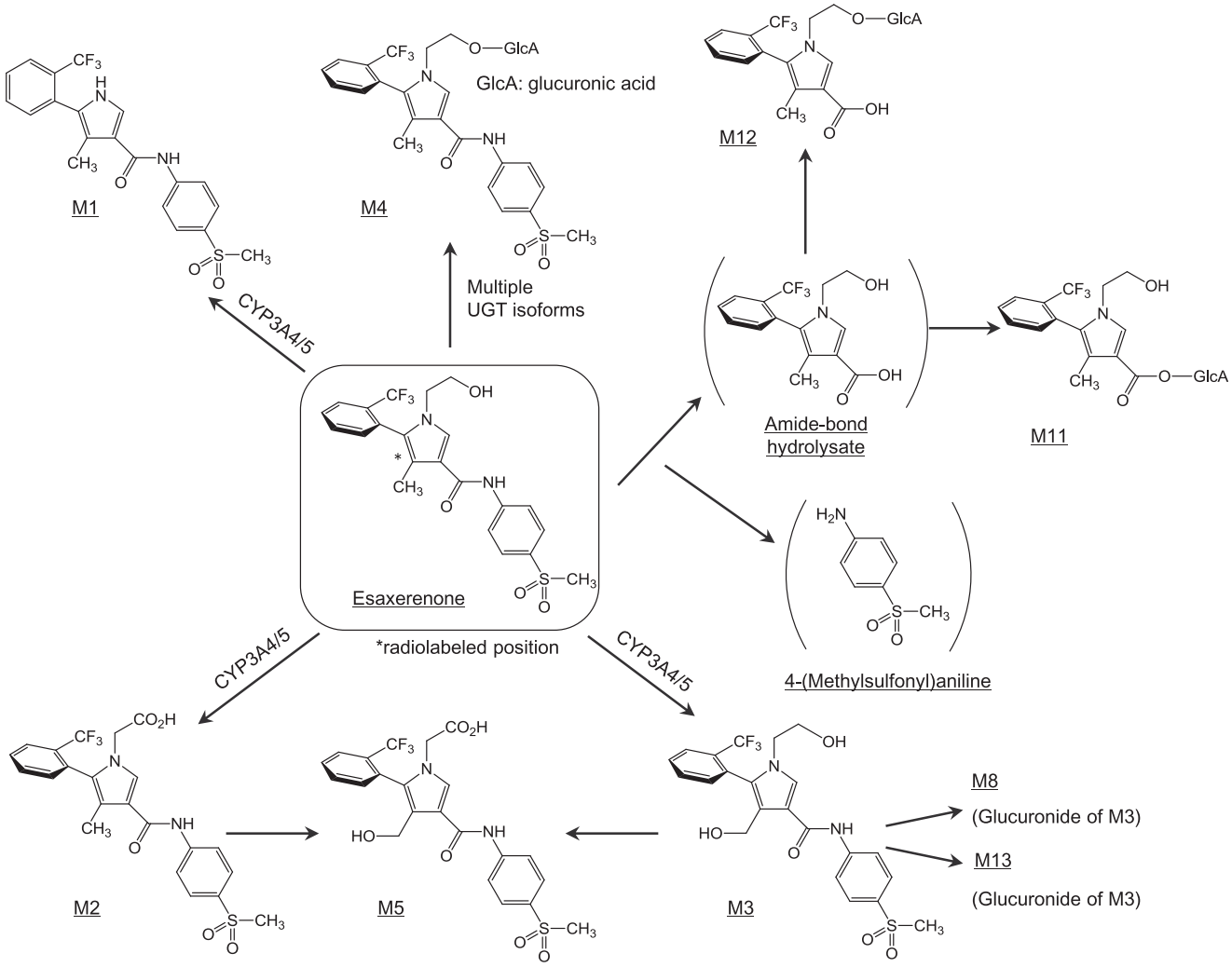


**Fig. 5.** Proposed major metabolic pathway of esaxerenone in humans. The structures of M1, M2, M3, M4, M5, and M11 were validated against authentic standards. The structures of other metabolites were proposed based on tandem mass spectrometry fragmentation and consistency with the validated metabolite structures. Some metabolites of which structures have not been identified are not included.

TABLE 4

Excretion of esaxerenone and its metabolites in urine and feces after oral administration of [$^{14}$C]esaxerenone

| Metabolite No. | Identification | Excretion Ratio | |
|---|---|---|---|
| | | Urine (0–72 h) | Feces (0–168 h) |
| | | % | % |
| | Esaxerenone | 1.6 | 18.7 |
| M2 | Carboxylic acid form | 2.6 | 9.0 |
| M3+M5 | Hydroxymethyl form + Hydroxymethyl-carboxylic acid form | 1.7 | 10.1 |
| M4 | *O*-glucuronide | 7.2 | — |
| M8 | Glucuronide of monooxygenated form | 1.6 | — |
| M11 | Glucuronide of amide-bond hydrolysate | 10.5 | — |
| M12 | *O*-glucuronide of amide-bond hydrolysate | 2.5 | — |
| M13 | Glucuronide of monooxygenated form | 1.3 | — |
| M15 | Sulfonic acid form | — | 0.9 |
| M16 | Dioxygenated form | — | 1.6 |
| M17 | Dioxygenated form | — | 1.0 |
| Others | (Sum of other unknown small peaks) | 4.8 | 9.8 |
| Total radioactivity | | 33.8 | 51.0 |

—, not detected.

following administration of 5 mg. Following oral administration, more than 90% of the dosed radioactivity was recovered in urine and feces by 288 hours postdose. The half-lives of the radioactivity in blood and plasma were similar to that of the unchanged form, and the value obtained by dividing blood $AUC_{last}$ by plasma $AUC_{last}$ was 0.628, suggesting low partitioning of esaxerenone and its major metabolites into blood components.

The fecal excretion of the unchanged esaxerenone was 18.7%. Assuming that all metabolism occurs after absorption, the absorption ratio ($F_a$) was considered to be at least 80%. Some drugs are metabolized by intestinal microbiota; however, this is unlikely for esaxerenone because the major metabolites observed in feces were oxidized forms. In monkeys, *O*-glucuronide (M4), a major metabolite in bile, was not detected in feces, suggesting that the glucuronide was hydrolyzed back to the unchanged form by the intestinal flora (Yamada et al., 2017). Because a similar phenomenon is likely to occur in humans, the $F_a$ was expected to be over 80%, and a high bioavailability, similar to rats (~100%) and monkeys (~70%), was expected. The high $F_a$ of esaxerenone was also suggested by the experiments using a Caco-2 cell monolayer (Fig. 7). When P-gp and BCRP inhibitors were added, the membrane permeability of esaxerenone was similar to that of theophylline, the $F_a$ of which is 100% of the dose in humans (Li et al., 2007). Given the high $F_a$, the DDI risk of esaxerenone and P-gp/BCRP inhibitors was expected to be low, although in vitro experiments indicated that esaxerenone was a substrate for these transporters.

The low excretion ratio of unchanged form in urine and feces suggested that esaxerenone was mainly cleared by metabolism. Metabolite profiling detected several oxidized forms, *O*-glucuronide, and glucuronides of amide-bond hydrolysate, which suggested esaxerenone has multiple metabolic pathways: oxidation, glucuronidation, and hydrolysis. To estimate the contribution of oxidative metabolism, the excretion ratio of the oxidized metabolites (M2, M3, M5, M16, and M17), and the metabolites for which the initial reaction is oxidation (M8 and M13) was summed. Approximately 30% of total body clearance was considered to result from oxidation. Among the oxidized metabolites, production of M1, M2, and M3 with CYP3A4 and CYP3A5 was confirmed in in vitro studies (Fig. 5A; Supplemental Fig. 2). However, even assuming that esaxerenone was completely oxidized only by CYP3A, the decrease in total body clearance by a strong CYP3A inhibitor was estimated to be approximately 30%. In contrast, eplerenone, a marketed MR blocker, is mostly metabolized by CYP3A, and the strong CYP3A inhibitor ketoconazole and the moderate inhibitors erythromycin and fluconazole increased its AUC by 5.39, 2.87, and 2.24 times, respectively (Cook et al., 2004). For this reason, eplerenone is contraindicated with strong CYP3A inhibitors, and dose reduction is required when used concomitantly with moderate CYP3A inhibitors, as written in the INSPRA product label (https://www.accessdata.fda.gov/drugsatfda_docs/label/2002/21437lbl.pdf). Esaxerenone is less susceptible to interactions with CYP3A inhibitor than eplerenone, making it favorable as a drug for the treatment of chronic diseases such as hypertension and diabetes.

M11 and M12 were glucuronides of amide-bond hydrolysate of esaxerenone. Further in vitro studies indicated that the hydrolysis occurred independent of NADPH in human liver microsomes, and did not occur in human plasma and liver cytosols (data not shown). The hydrolysis in human liver microsomes was inhibited by several esterase inhibitors: bis-p-nitrophenyl phosphate, phenylmethylsulfonyl fluoride, eserine, diisopropylfluoro phosphate, and p-chloromercuribenzoate (data not shown). The involved enzyme is still unknown; however, the possibility of interaction via hydrolysis was low because the sum of the excretion ratio of M11 and M12 was approximately 13%. The calculation of the contribution of *O*-glucuronic acid is difficult because *O*-glucuronide (M4) is returned to the unchanged form in the intestinal lumen after biliary excretion. Nevertheless, the DDI risk via UGT was considered to be low, since multiple UGT isoforms were involved in the glucuronidation of esaxerenone (Fig. 6B), and the complete inhibition of all isoforms is unlikely. Multiple UGT isoforms were also involved in the glucuronidation of 1-(2-hydroxyethyl)-4-methyl-5-[2-(trifluoromethyl)phenyl]-1*H*-pyrrole-3-carboxylic acid, a hydrolyzed form of esaxerenone (data not shown). The formation of M15, a sulfonic acid form, can be explained by initial oxidative demethylation of the methylsulfonyl moiety to generate a sulfinic acid intermediate, followed by oxidative conversion to sulfonic acid. This unusual metabolic pathway from methyl sulfone to sulfonic acid has been reported previously for odanacatib (Kassahun et al., 2011).

The urinary excretion of the unchanged esaxerenone in human was as low as 1.6%, suggesting the low contribution of renal clearance to the total body clearance of esaxerenone. Therefore, the DDI potential via inhibition of renal transporters, such as organic anion transporters, organic cation transporters, and multidrug and toxin extrusion transporters, is considered to be low. Furthermore, low urinary excretion suggested that the plasma exposure of esaxerenone was not affected by renal dysfunction. This property was preferable since esaxerenone is

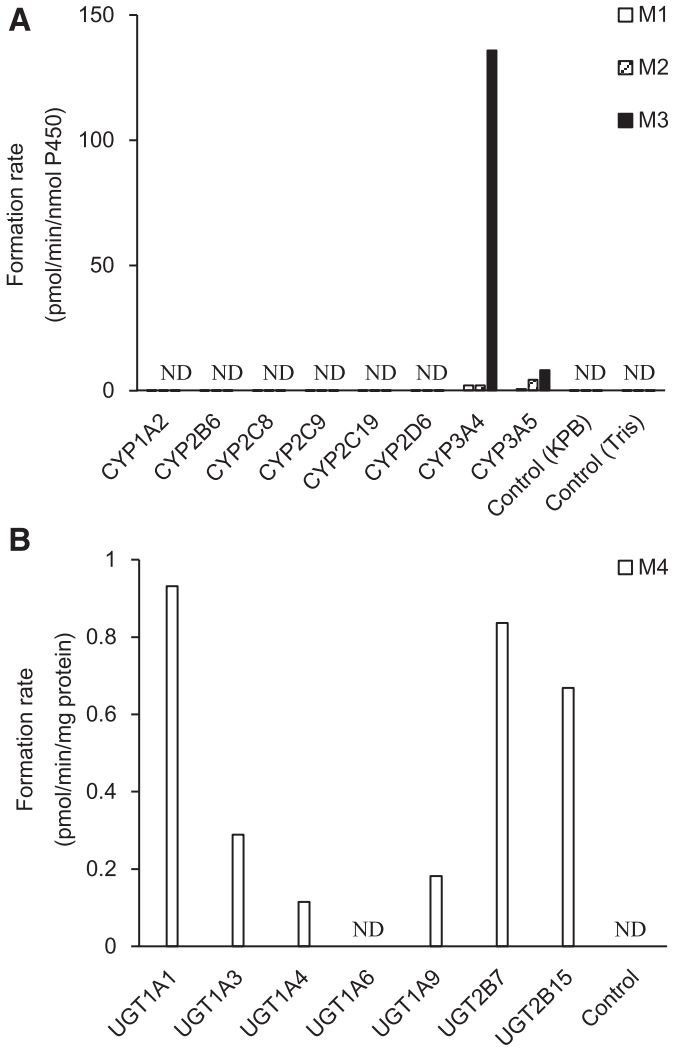


**Fig. 6.** Formation rates of the metabolites from esaxerenone in microsomes expressing human P450 isoforms (A) and UGT isoforms (B). Control (KPB) indicates control microsomes in potassium phosphate buffer and Control (Tris) indicates control microsomes in Tris buffer. ND indicates not detected.

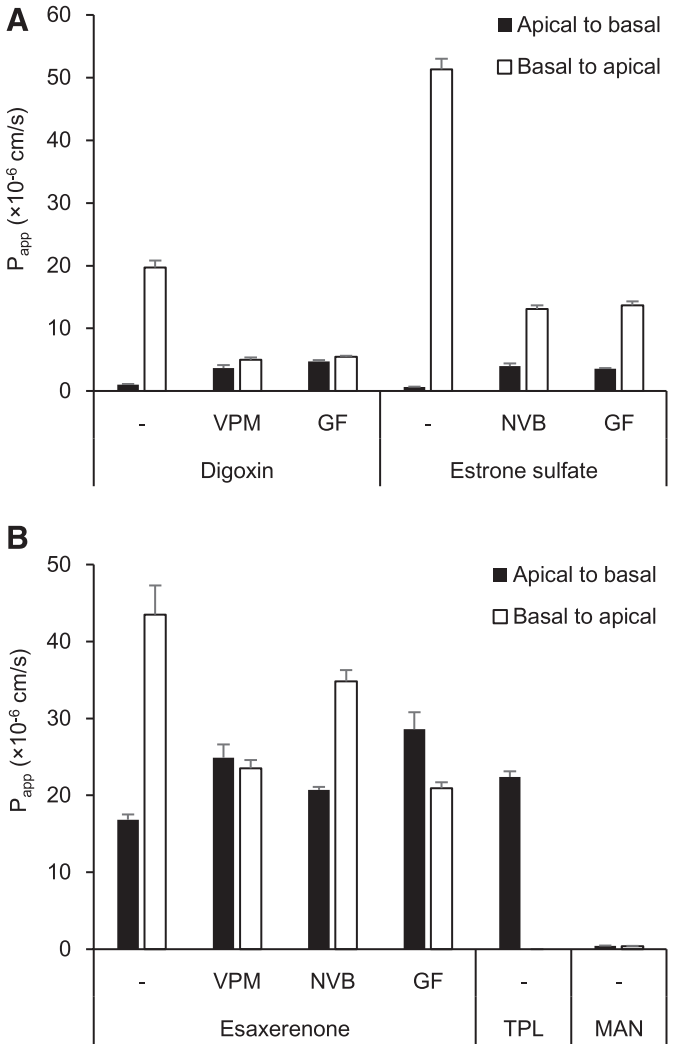


**Fig. 7.** Transcellular transport across Caco-2 cell monolayers and the effect of verapamil [(VPM), P-gp inhibitor], novobiocin [(NVB), BCRP inhibitor], and GF120918 [(GF), P-gp and BCRP inhibitor] of digoxin and estrone sulfate (A); esaxerenone, theophylline (TPL), and mannitol (MAN) (B). The minus sign indicates no inhibitor.

expected to be administered to patients with renal impairment, such as hypertension, chronic kidney disease, and type 2 diabetes with microalbuminuria.

Quantification of circulating metabolites is necessary to evaluate their potential toxicity risk. The results of the radio/high-performance liquid chromatography analysis showed that unchanged esaxerenone was the major component in plasma, and that the *O*-glucuronide of esaxerenone (M4) and the acyl-glucuronide of amide-bond hydrolysate (M11) were detected as circulating metabolites. The metabolite/radioactivity AUCR of M4 was slightly high (21.4%); however, according to the guidance on metabolites in safety testing, conjugated metabolites such as *O*-glucuronide are usually less pharmacologically active, so no additional evaluation is required (Food and Drug Administration, 2016). Furthermore, M4 was also a major metabolite in monkey plasma (Yamada et al., 2017), and its concentration in the toxicity study was considered to be higher than that in humans (data not shown). Although the deshydroxyethyl form (M1) was not observed on the radiochromatogram, its plasma concentration was measured by LC-MS/MS because it showed a weak antagonistic effect on MR and its half-life was much longer than that of the unchanged form in nonclinical studies (data not shown). As predicted, M1 was eliminated very slowly from human plasma; therefore, its AUCR (1.7%) was calculated by using $AUC_{last}$ instead of $AUC_{inf}$. Owing to its long $t_{1/2}$, the steady-state AUCR of M1 was undetermined; however, it was considered to be less than 10% of total radioactivity exposure since the metabolite-to-parent trough concentration ratio was less than 10% at steady state after 6-week administration of esaxerenone to hypertension patients (data on file).

The AUCR of M11 was not very high (8.0%). Although M11 was not detected in rat and monkey plasma in a previous study (Yamada et al., 2017), it was detected in the toxicity study samples (100 mg/kg for rats and 1000 mg/kg for monkeys) by quantitative LC-MS/MS analysis. The AUC of M11 in rat and monkey plasma was approximately half of that observed in human plasma in the current study (data on file). Considering the dosing amount in the current study was higher than the clinical dose, the exposures in animals are suggested to support those in humans.

The existence of M11 and M12 suggests the exposure of the complementary part, 4MSA, in the human body; however, 4MSA and its metabolites were not detected on the radiochromatogram since this moiety was not radiolabeled. Since the hydrolyzed metabolite was not observed in rats and monkeys, further nonclinical evaluation is difficult,

even if another [$^{14}$C]esaxerenone with labeled 4MSA was synthesized. Therefore, [$^{14}$C]4MSA was synthesized and administered intravenously to rats to investigate its fate. The results indicated that 4MSA was metabolized to the acetylated form, and the radioactivity was excreted mainly into urine (Supplemental Fig. 2). The $t_{1/2}$ of the radioactivity after the administration of [$^{14}$C]4MSA was approximately 6.5 hours and was similar to that of esaxerenone administered to rats (Yamada et al., 2017), suggesting a low possibility of accumulation of 4MSA and its metabolites. Furthermore, when the concentrations of 4MSA and its metabolites were measured in plasma from healthy volunteers after administration of 5 mg esaxerenone for 14 days, their AUC was less than 3% of that of the unchanged esaxerenone (data not shown).

In conclusion, because of the high absorption ratio and various metabolic pathways involved, the DDI potential of esaxerenone with enzyme inhibitors was considered to be limited. The low urinary excretion of unchanged esaxerenone suggested that the contribution of renal clearance was limited and that renal impairment did not significantly affect esaxerenone exposure. The exposure of the metabolites of esaxerenone in human plasma was evaluated, and it was confirmed that they were covered with nonclinical toxicity studies. These characteristics are considered to demonstrate its favorability for clinical use.

**Acknowledgments**

We thank Worldwide Clinical Trials for conducting the clinical study, Celerion for conducting the bioanalysis, and LSI Medience Corporation (Tokyo, Japan) for conducting the metabolite analysis. We also thank Dr. M. Honzumi, Dr. Y. Asoh, Dr. H. Tsuruoka, and Dr. K. Aoki from Daiichi Sankyo for the preparation of the authentic standard of the metabolites, and Dr. M. Kotsuma from Daiichi Sankyo Pharma Development for kind support.

**Authorship Contributions**

*Participated in research design:* Yamada, Mendell, Takakusa, Shimizu.

*Conducted experiments:* Yamada, Takakusa.

*Performed data analysis:* Yamada, Mendell, Takakusa.

*Wrote or contributed to the writing of the manuscript:* Yamada, Takakusa, Mendell, Shimizu, Ando.

**References**

Aoki K, Tsuruoka H, Hayashi N, Yoshida J, and Asoh Y (2008) inventors, Daiichi Sankyo Co. Ltd., assignee. Atropisomer of pyrrole derivative. WO2008126831A1. 2008 Oct 23.

Arai K, Homma T, Morikawa Y, Ubukata N, Tsuruoka H, Aoki K, Ishikawa H, Mizuno M, and Sada T (2015a) Pharmacological profile of CS-3150, a novel, highly potent and selective non-steroidal mineralocorticoid receptor antagonist. *Eur J Pharmacol* **761**:226–234.

Arai K, Morikawa Y, Ubukata N, Tsuruoka H, and Homma T (2016) CS-3150, a novel non-steroidal mineralocorticoid receptor antagonist, shows preventive and therapeutic effects on renal injury in deoxycorticosterone acetate/salt-induced hypertensive rats. *J Pharmacol Exp Ther* **358**: 548–557.

Arai K, Tsuruoka H, and Homma T (2015b) CS-3150, a novel non-steroidal mineralocorticoid receptor antagonist, prevents hypertension and cardiorenal injury in Dahl salt-sensitive hypertensive rats. *Eur J Pharmacol* **769**:266–273.

Brem AS, Morris DJ, and Gong R (2011) Aldosterone-induced fibrosis in the kidney: questions and controversies. *Am J Kidney Dis* **58**:471–479.

Canne Bannen L, Chen J, Dalrymple LE, Flatt BT, Forsyth TP, Gu XH, Mac MB, Mann LW, Mann G, Martin R, et al. (2006) inventors, Exelixis, Inc., assignee. Pyrrole derivatives as pharmaceutical agents. WO2006012642A2. 2006 Feb 2.

Cook CS, Berry LM, and Burton E (2004) Prediction of in vivo drug interactions with eplerenone in man from in vitro metabolic inhibition data. *Xenobiotica* **34**:215–228.

Epstein M, Williams GH, Weinberger M, Lewin A, Krause S, Mukherjee R, Patni R, and Beckerman B (2006) Selective aldosterone blockade with eplerenone reduces albuminuria in patients with type 2 diabetes. *Clin J Am Soc Nephrol* **1**:940–951.

Food and Drug Administration (2016) *Guidance for Industry: Safety Testing of Drug Metabolites*, US Department of Health and Human Services Center for Drug Evaluation and Research, FDA, Silver Spring, MD.

Funder JW (1995) Mineralocorticoid receptors and hypertension. *J Steroid Biochem Mol Biol* **53**:53–55.

Kassahun K, Black WC, Nicoll-Griffith D, McIntosh I, Chauret N, Day S, Rosenberg E, and Koeplinger K (2011) Pharmacokinetics and metabolism in rats, dogs, and monkeys of the cathepsin K inhibitor odanacatib: demethylation of a methylsulfonyl moiety as a major metabolic pathway. *Drug Metab Dispos* **39**:1079–1087.

Kato M, Furuie H, Shimizu T, Miyazaki A, Kobayashi F, and Ishizuka H (2018) Single- and multiple-dose escalation study to assess pharmacokinetics, pharmacodynamics and safety of oral esaxerenone in healthy Japanese subjects. *Br J Clin Pharmacol* **84**:1821–1829.

Li C, Liu T, Cui X, Uss AS, and Cheng KC (2007) Development of in vitro pharmacokinetic screens using Caco-2, human hepatocyte, and Caco-2/human hepatocyte hybrid systems for the prediction of oral bioavailability in humans. *J Biomol Screen* **12**:1084–1091.

Lombès M, Alfaidy N, Eugene E, Lessana A, Farman N, and Bonvalet JP (1995) Prerequisite for cardiac aldosterone action. Mineralocorticoid receptor and 11 $\beta$-hydroxysteroid dehydrogenase in the human heart. *Circulation* **92**:175–182.

Nagai Y, Miyata K, Sun GP, Rahman M, Kimura S, Miyatake A, Kiyomoto H, Kohno M, Abe Y, Yoshizumi M, et al. (2005) Aldosterone stimulates collagen gene expression and synthesis via activation of ERK1/2 in rat renal fibroblasts. *Hypertension* **46**:1039–1045.

Nishiyama A, Yao L, Fan Y, Kyaw M, Kataoka N, Hashimoto K, Nagai Y, Nakamura E, Yoshizumi M, Shokoji T, et al. (2005) Involvement of aldosterone and mineralocorticoid receptors in rat mesangial cell proliferation and deformability. *Hypertension* **45**:710–716.

Patni H, Mathew JT, Luan L, Franki N, Chander PN, and Singhal PC (2007) Aldosterone promotes proximal tubular cell apoptosis: role of oxidative stress. *Am J Physiol Renal Physiol* **293**:F1065–F1071.

Pitt B, Remme W, Zannad F, Neaton J, Martinez F, Roniker B, Bittman R, Hurley S, Kleiman J, and Gatlin M; Eplerenone Post-Acute Myocardial Infarction Heart Failure Efficacy and Survival Study Investigators (2003) Eplerenone, a selective aldosterone blocker, in patients with left ventricular dysfunction after myocardial infarction. *N Engl J Med* **348**:1309–1321.

Pitt B, Zannad F, Remme WJ, Cody R, Castaigne A, Perez A, Palensky J, and Wittes J; Randomized Aldactone Evaluation Study Investigators (1999) The effect of spironolactone on morbidity and mortality in patients with severe heart failure. *N Engl J Med* **341**:709–717.

Rautio J, Humphreys JE, Webster LO, Balakrishnan A, Keogh JP, Kunta JR, Serabjit-Singh CJ, and Polli JW (2006) In vitro P-glycoprotein inhibition assays for assessment of clinical drug interaction potential of new drug candidates: a recommendation for probe substrates. *Drug Metab Dispos* **34**:786–792.

Rose LI, Underwood RH, Newmark SR, Kisch ES, and Williams GH (1977) Pathophysiology of spironolactone-induced gynecomastia. *Ann Intern Med* **87**:398–403.

Rossing K, Schjoedt KJ, Smidt UM, Boomsma F, and Parving HH (2005) Beneficial effects of adding spironolactone to recommended antihypertensive treatment in diabetic nephropathy: a randomized, double-masked, cross-over study. *Diabetes Care* **28**:2106–2112.

Saruta T, Kageyama S, Ogihara T, Hiwada K, Ogawa M, Tawara K, Gatlin M, Garthwaite S, Bittman R, and Patrick J (2004) Efficacy and safety of the selective aldosterone blocker eplerenone in Japanese patients with hypertension: a randomized, double-blind, placebo-controlled, dose-ranging study. *J Clin Hypertens (Greenwich)* **6**:175–183, quiz 184–185.

Shibata S, Nagase M, Yoshida S, Kawachi H, and Fujita T (2007) Podocyte as the target for aldosterone: roles of oxidative stress and Sgk1. *Hypertension* **49**:355–364.

Siragy HM and Xue C (2008) Local renal aldosterone production induces inflammation and matrix formation in kidneys of diabetic rats. *Exp Physiol* **93**:817–824.

Weinberger MH, Roniker B, Krause SL, and Weiss RJ (2002) Eplerenone, a selective aldosterone blocker, in mild-to-moderate hypertension. *Am J Hypertens* **15**:709–716.

Xia CQ, Yang JJ, and Gan LS (2005) Breast cancer resistance protein in pharmacokinetics and drug-drug interactions. *Expert Opin Drug Metab Toxicol* **1**:595–611.

Yamada M, Takei M, Suzuki E, Takakusa H, Kotsuma M, Washio T, Murayama N, Inoue SI, and Izumi T (2017) Pharmacokinetics, distribution, and disposition of esaxerenone, a novel, highly potent and selective non-steroidal mineralocorticoid receptor antagonist, in rats and monkeys. *Xenobiotica* **47**:1090–1103.

**Address correspondence to:** Makiko Yamada, Drug Metabolism and Pharmacokinetics Research Laboratories, Daiichi Sankyo Co., Ltd., 1-2-58, Hiromachi, Shinagawa-ku, Tokyo 140-8710, Japan. E-mail: yamada.makiko.jr@daiichisankyo.co.jp

**Supplemental Data**

# Pharmacokinetics, Metabolism, and Excretion of [$^{14}$C]Esaxerenone, a Novel Mineralocorticoid Receptor Blocker in Humans

Makiko Yamada, Jeanne Mendell, Hideo Takakusa, Takako Shimizu, Osamu Ando

*Drug Metabolism and Pharmacokinetics Research Laboratories (M.Y., H.S., O.A.) and Clinical Pharmacology Department (T.S.), Daiichi Sankyo Co., Ltd., Tokyo, Japan; and Daiichi Sankyo Pharma Development, Basking Ridge, NJ, USA (J.M.)*

## Supplemental methods

### Analysis of Total Radioactivity, Esaxerenone, and Metabolite Concentration

Plasma esaxerenone and metabolite concentrations were measured by a validated liquid chromatography-tandem mass spectrometry (LC-MS/MS) assay at Celerion (Lincoln, NE) using an electrospray ionization (ESI) interface in the positive ion mode. Chromatographic separation was carried out in the analytical column of an ACE C18 (50 × 2.1 mm, 5 µm, 100 Å, Advanced chromatography technologies, Aberdeen, Scotland) with ambient temperature. The autosampler temperature was maintained at 4°C. When the concentration of esaxerenone was measured, the analytes were extracted using a liquid-liquid extraction procedure. Briefly, 0.1 mL of plasma sample, 0.05 mL of deuterium-labeled esaxerenone solution (5 ng/mL in 50% acetonitrile), 0.1 mL of 50% acetonitrile, and 0.1 mL of 2% ammonium hydroxide were mixed, and 1 mL of n-butyl chloride was added and mixed. The top organic layer was collected and evaporated to dryness under a gentle stream of nitrogen gas, reconstituted with 20% acetonitrile and then injected into the LC-MS/MS. The mobile phase of acetonitrile/methanol/20 mM ammonium formate/heptafluorobutyric acid (30/35/35/0.01, v/v/v/v) was set at the flow-rate of 0.5 mL/min. Mass spectrometric detection was performed on an API 4000 (AB Sciex, Framingham, MA), and the multiple reaction monitoring (MRM) transitions monitored for esaxerenone and deuterium-labeled esaxerenone were *m/z* 467.1 to 270.1 and 474.2 to 274.1, respectively. When the concentration of M1 was measured, 0.1 mL of plasma sample, 0.025 mL of deuterium-labeled M1 solution (2.5 ng/mL in acetonitrile), and 0.1 mL of 50 mM ammonium formate (pH 10.0, adjusted with ammonium hydroxide) were mixed and extracted similarly to esaxerenone. The mobile phase consisted of two solvents: A (10% acetonitrile) and B (90% acetonitrile) delivered at a flow-rate of 0.8 mL/min. The mobile phase composition started at 40% B and was maintained for 0.1 min, followed by a linear increase to

70% B from 0.1 to 3 min, and then returned to the initial running condition (40% B) by a linear decrease from 3 to 3.5 min. Mass spectrometric detection was performed on an API 4000, and the MRM transitions monitored for M1 and deuterium-labeled M1 were m/z 423.5 to 226.2 and 426.5 to 226.2, respectively. When the concentration of M4 was measured, 0.05 mL of plasma sample, 0.05 mL of deuterium-labeled esaxerenone solution (5 ng/mL in 50% acetonitrile), and 0.35 mL of acetonitrile were mixed and centrifuged. The top organic layer was collected and evaporated to dryness under a gentle stream of nitrogen gas, reconstituted with 20% acetonitrile, and then injected into the LC-MS/MS. The mobile phase of 40% acetonitrile containing 0.1% formic acid was set at the flow-rate of 0.5 mL/min. Mass spectrometric detection was performed on an API 5000 (AB Sciex), and the MRM transitions monitored for M4 was *m/z* 643.3 to 270.0. When the concentration of M11 was measured, 0.25 mL of plasma containing analyte, 0.04 mL of deuterium-labeled esaxerenone solution (5000 ng/mL in 25% methanol), and 0.5 mL of 100 mM ammonium acetate were mixed, 0.7 mL of ultrapure water was added and mixed, and then extracted using a solid phase extraction plates (OASIS HLB 60 mg, Waters). The eluates were evaporated to dryness, reconstituted with 0.05 mL of methanol, diluted with 0.2 mL of 25% methanol, filtered with 96 well filter plate (Millipore, MultiScreen-BV, 1.2 µm), and then injected into the LC-MS/MS. The mobile phase consisted of two solvents: A (20% acetonitrile containing 0.1% acetic acid) and B (acetonitrile containing 0.1% acetic acid) delivered at a flow-rate of 0.5 mL/min. Chromatographic separation was carried out in the analytical column of an ACQUITY UPLC HSS T3 (100 × 2.1 mm, 1.8 µm, Waters) with an oven temperature set at 50°C. Mass spectrometric detection was performed on an API 6500 (AB Sciex), and the MRM transitions monitored for M11 was *m/z* 295.9 to 232.0. After LC-MS/MS analysis, quantitation was determined using a weighted linear regression analysis ($1/\text{concentration}^2$) of peak area ratios of the analyte and internal standard.

### Preparation of biological samples for metabolite profiling

The plasma, urine, or fecal samples were mixed with a 2-fold volume of acetonitrile. The mixture was centrifuged (4°C, 21,500 × g, 5 min), and the resulting supernatant was collected. The precipitate was extracted again with the same volume of acetonitrile described above. The two batches of extracts were combined and concentrated under a nitrogen stream. To the resulting residue, 20% acetonitrile aqueous solution was added, and the mixture was stirred. The resulting solution was centrifuged to obtain the supernatant as a sample for metabolite profiling.

### Metabolite profiling of human plasma, urine, and feces

Chromatographic separation was achieved with an HPLC column (XBridge, 3.5 μm, 4.6 mm I.D. × 100 mm L, Waters Corp., Milford, MA) with a gradient program, which combined two solvents (A and B) at 40°C. Solvents A and B consisted 0.1% formic acid in purified water and 0.1% formic acid in acetonitrile, respectively. The HPLC flow-rate was 1.0 mL/min. The mobile phase composition started at 25% B and was maintained for 3 min, followed by a linear increase to 35% B from 5 to 30 min, followed by a linear increase to 95% B from 30 to 35 min. The gradient was kept at 95% B until 37 min and was then returned to the initial running condition. A portion (five-sixth volume) of the whole eluate from the HPLC (Accela, Thermo Fisher Scientific) was introduced into radioactivity detector (Radiomatic 625TR, PerkinElmer) to detect radioactive peaks, while the residual portion (one-sixth volume) was introduced into an MS detector (LTQ-Orbitrap XL; Thermo Fisher Scientific) with a splitter to identify metabolites. An Ultima-Flo M (PerkinElmer) was used as a scintillation cocktail for radioactivity detection. The ESI source of MS detector was set in negative ion mode, and the analytical conditions were set as follows: spray voltage, 5 kV; capillary voltage, −50 V; sheath gas flow, 40 arbitrary units;

aux gas flow, 20 arbitrary units; sweep gas flow, 3 arbitrary units; and capillary temperature, 300°C. MS/MS data were acquired in high-energy collisional dissociation (HCD) or collision-induced dissociation (CID) mode with the following collision energy: 100 arbitrary units for HCD and 35 eV for CID.

### In vitro identification of P450 isoform

Two studies were conducted to identify P450 isoforms involved in the oxidative metabolism of esaxerenone. For the recombinant study, the mixture containing each microsomes from baculovirus-infected insect cells expressing human cytochrome P450 (P450) isoforms (CYP1A2, CYP2B6, CYP2C8, CYP2C9, CYP2C19, CYP2D6, CYP3A4, and CYP3A5, final concentration: 30 pmol P450/mL), control microsomes for adjustment of the protein concentration (final concentration: 1 mg protein/mL), tris buffer (final concentration: 100 mM, pH 7.5) for CYP2C9 or potassium phosphate buffer (final concentration: 100 mM, pH 7.4) for other isoforms, and purified water were prepared as a reaction mixture. For the control experiment, only control microsomes were added to the reaction mixture. For the correlation analysis, the mixture containing each individual human liver microsome (final concentration: 1 mg protein/mL), potassium phosphate buffer (final concentration: 100 mM, pH 7.4), and purified water was prepared as a reaction mixture. NADPH regeneration system solution A, NADPH regeneration system solution B, and purified water were mixed to prepare NADPH regeneration system (NADPHgs). The incubation was carried out in duplicate. An aliquot esaxerenone solution was added to the reaction mixture (final concentration: 10 μM). After pre-warming the mixture at 37°C for approximately 5 min, a reaction was started by the addition of NADPHgs. After incubation at 37°C for 15 min (for M2 and M3) and 60 min (for M1), a portion of the incubation mixture was added to acetonitrile/methanol (3/1, v/v) containing deuterium-labeled M1 to stop

the reaction. These mixtures were filtered by Captiva (Agilent Technologies, Santa Clara, CA), and the concentrations of M1, M2, and M3 were measured by an LC-MS/MS method.

### Transcellular transport across Caco-2 cell via P-gp and BCRP

To evaluate the transcellular transport via P-glycoprotein (P-gp) and breast cancer resistance protein (BCRP), Caco-2 cells were seeded at a density of $1\times10^5$ cells/cm$^2$ in 48 well plates (Culture Insert; PET porous filter; pore size, 1 μm; area, 0.3 cm$^2$; and Cell Culture Insert Companion Plate, Corning). The cells were incubated at 37°C in a $CO_2$ incubator ($CO_2$: 5%) for 22 days. DMEM containing FBS, non-essential amino acid, L-glutamine, and antibiotic-antimycotic was used as culture medium. On the day of the experiment, the transepithelial electrical resistance was measured to check the integrity of the monolayer using Millicell-ERS (Merck Millipore, Billerica, MA).

For the bidirectional transport assay, the medium at the apical side (300 μL) and basal side (1000 μL) of the plate was removed by aspiration and replaced with HBSS or HBSS containing verapamil (typical P-gp inhibitor, 100 μM), novobiocin (typical BCRP inhibitor, 10 μM), or GF120918 (P-gp and BCRP inhibitor, 10 μM), and the plate was preincubated at 37°C for 1 h. After the preincubation, the solution in the donor side was replaced with HBSS buffer containing 1 μM of [$^{14}$C]esaxerenone (with or without inhibitors), 1 μM of [$^3$H]digoxin (typical P-gp substrate, with or without inhibitors), 0.1 μM of [$^3$H]estrone sulfate (typical BCRP substrate, with or without inhibitors), 10 μM of [$^{14}$C]theophylline (high permeability marker), or 10 μM of [$^{14}$C]mannitol (low permeability marker). The solution in the receiver side was replaced with the same buffer as pre-incubation. The concentration of DMSO was 0.2% for all of the incubation conditions. After incubation for a designated period (0.5, 1, and 2 h for esaxerenone, and 2 h for others) at 37°C, the receiver side solution (100 μL) was collected into a

glass vial. In order to compensate for the volume sampled at 0.5 and 1 h, 100 µL of assay solution was added to the receiver side of the esaxerenone wells. The assay solution (10 µL) was collected from the donor side at 1 h as a donor side and the radioactivity was counted using LSC. Incubation was performed in triplicate.

**Supplemental Figure 1** Fragmentation schemes of esaxerenone and its metabolites.

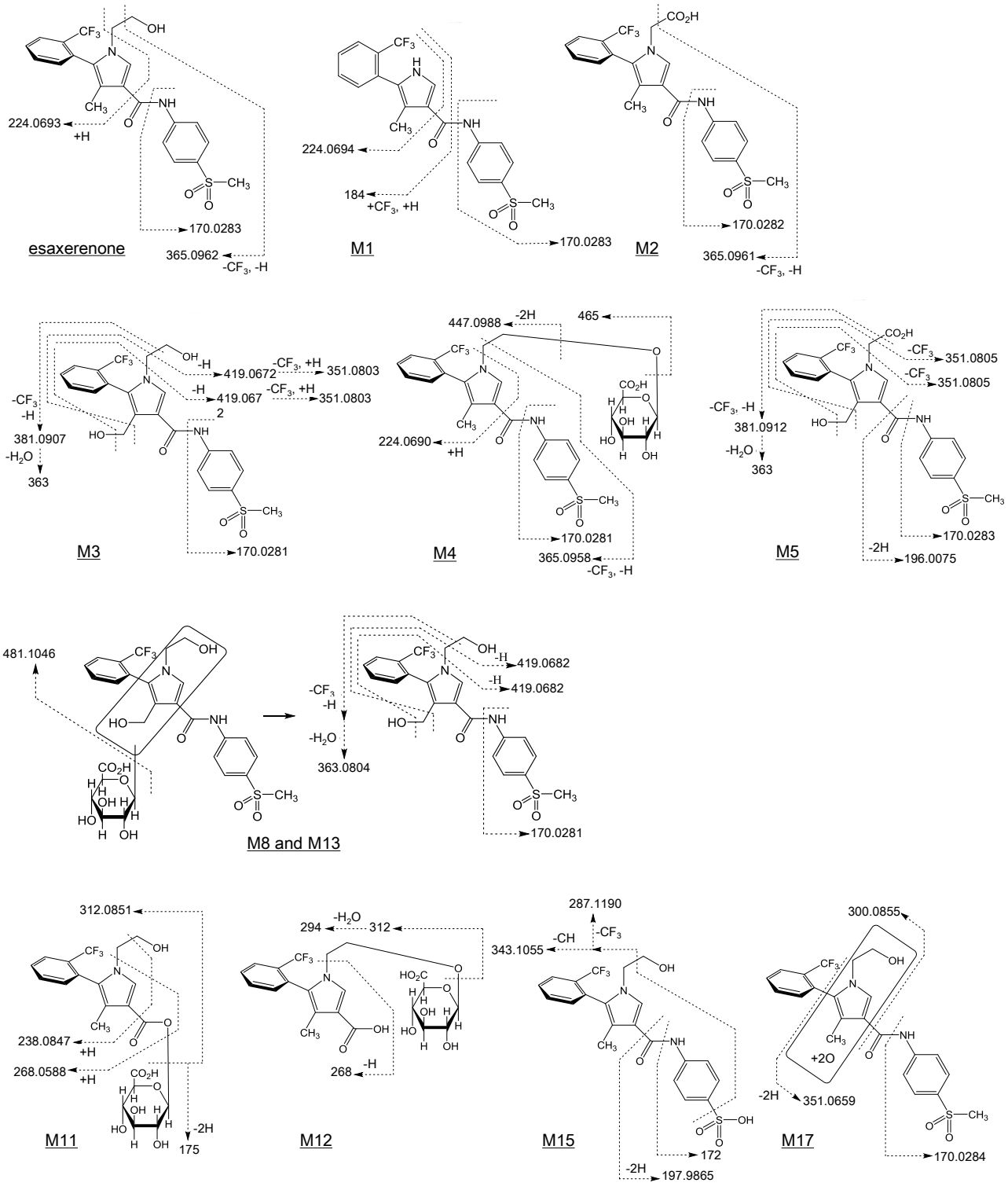

**Supplemental Figure 2** Correlation between the formation rate of M1, M2, and M3, and the P450 isoform activity in individual human liver microsomes. CYP3A4/5(T) indicates a correlation with testosterone 6β-hydroxylation activity, and CYP3A4/5(M) indicates a correlation with midazolam 1'-hydroxylation activity.

M1

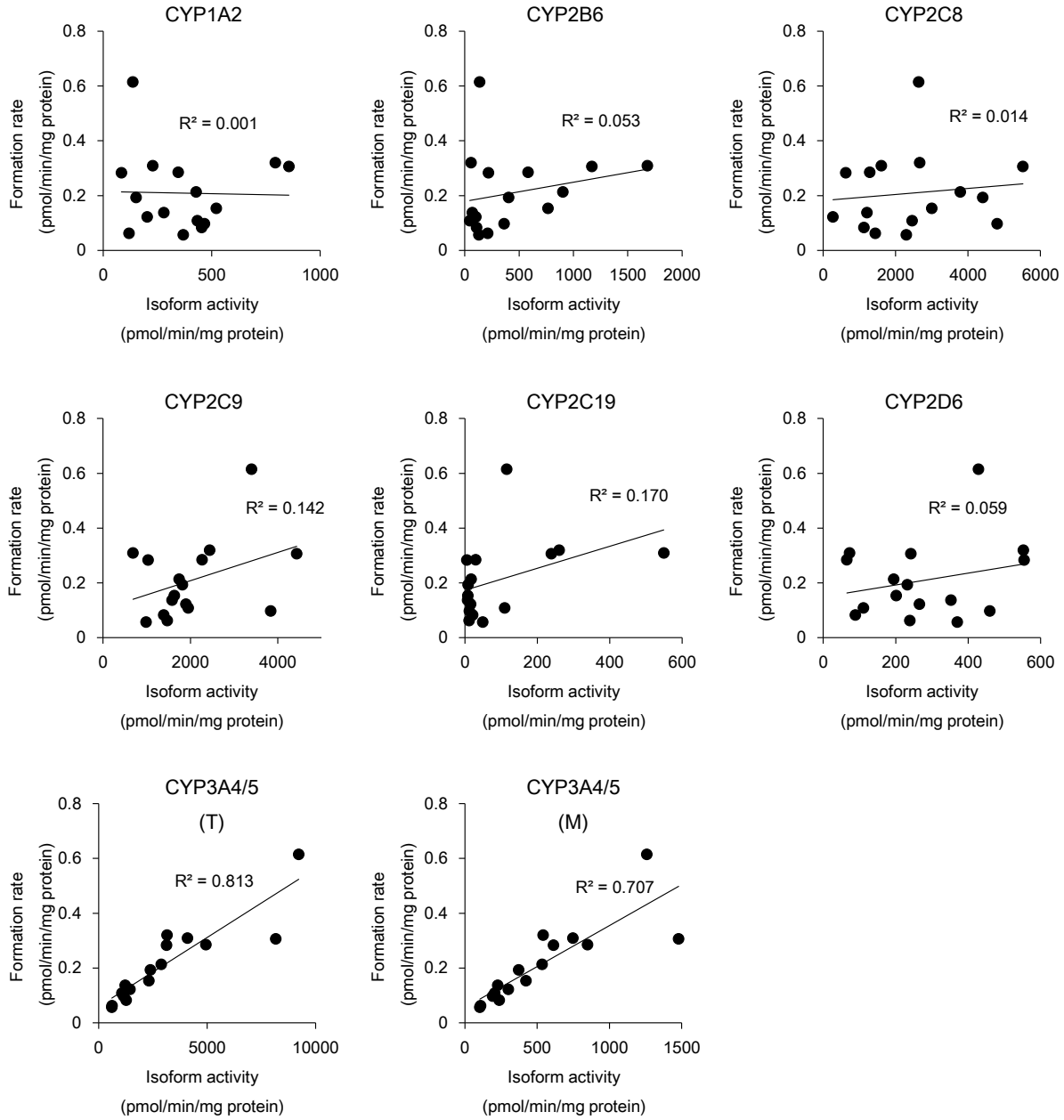

M2

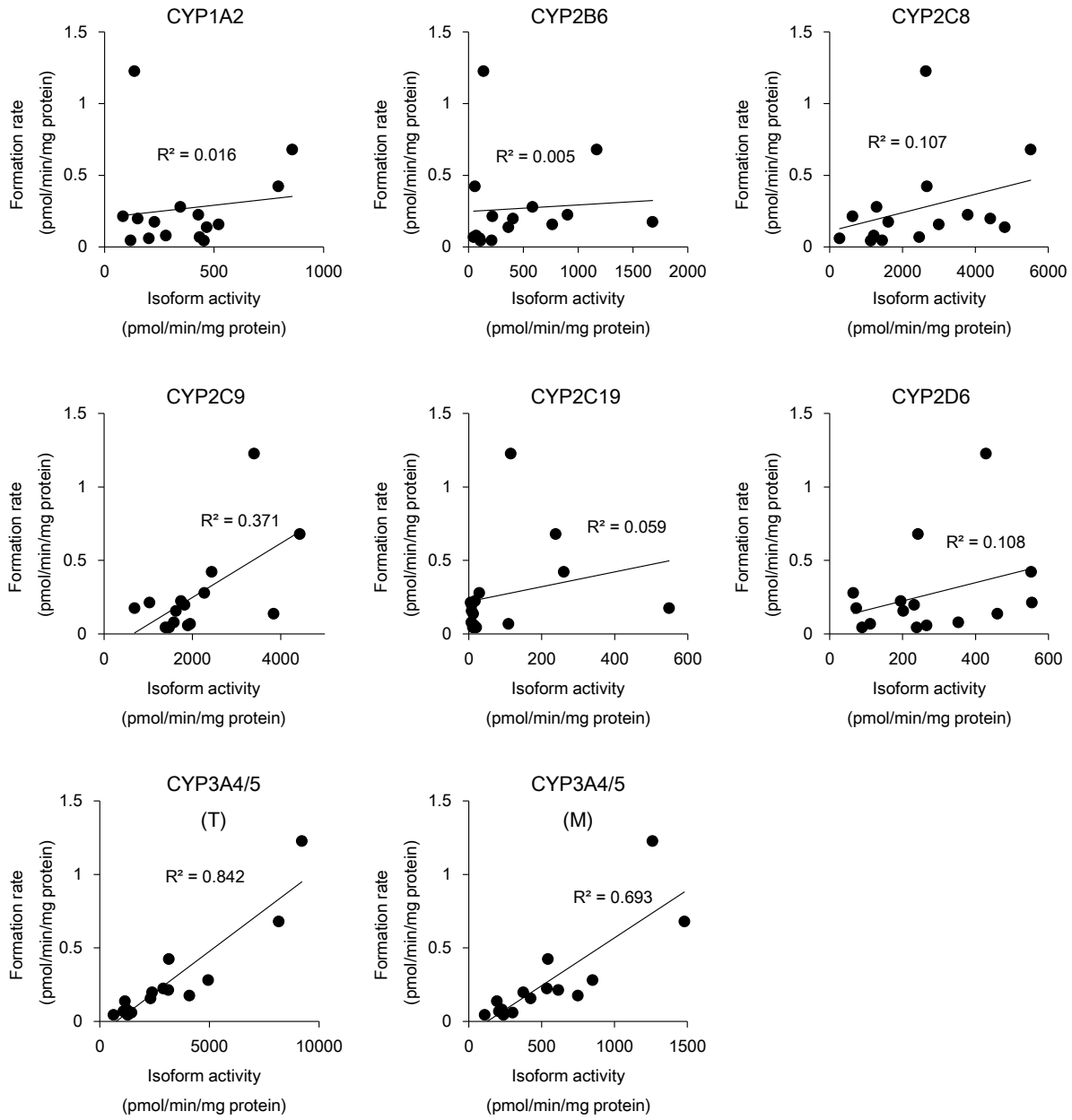
CYP1A2
R² = 0.016
CYP2B6
R² = 0.005
CYP2C8
R² = 0.107
CYP2C9
R² = 0.371
CYP2C19
R² = 0.059
CYP2D6
R² = 0.108
CYP3A4/5
(T)
R² = 0.842
CYP3A4/5
(M)
R² = 0.693
Formation rate
(pmol/min/mg protein)
Isoform activity
(pmol/min/mg protein)

M3

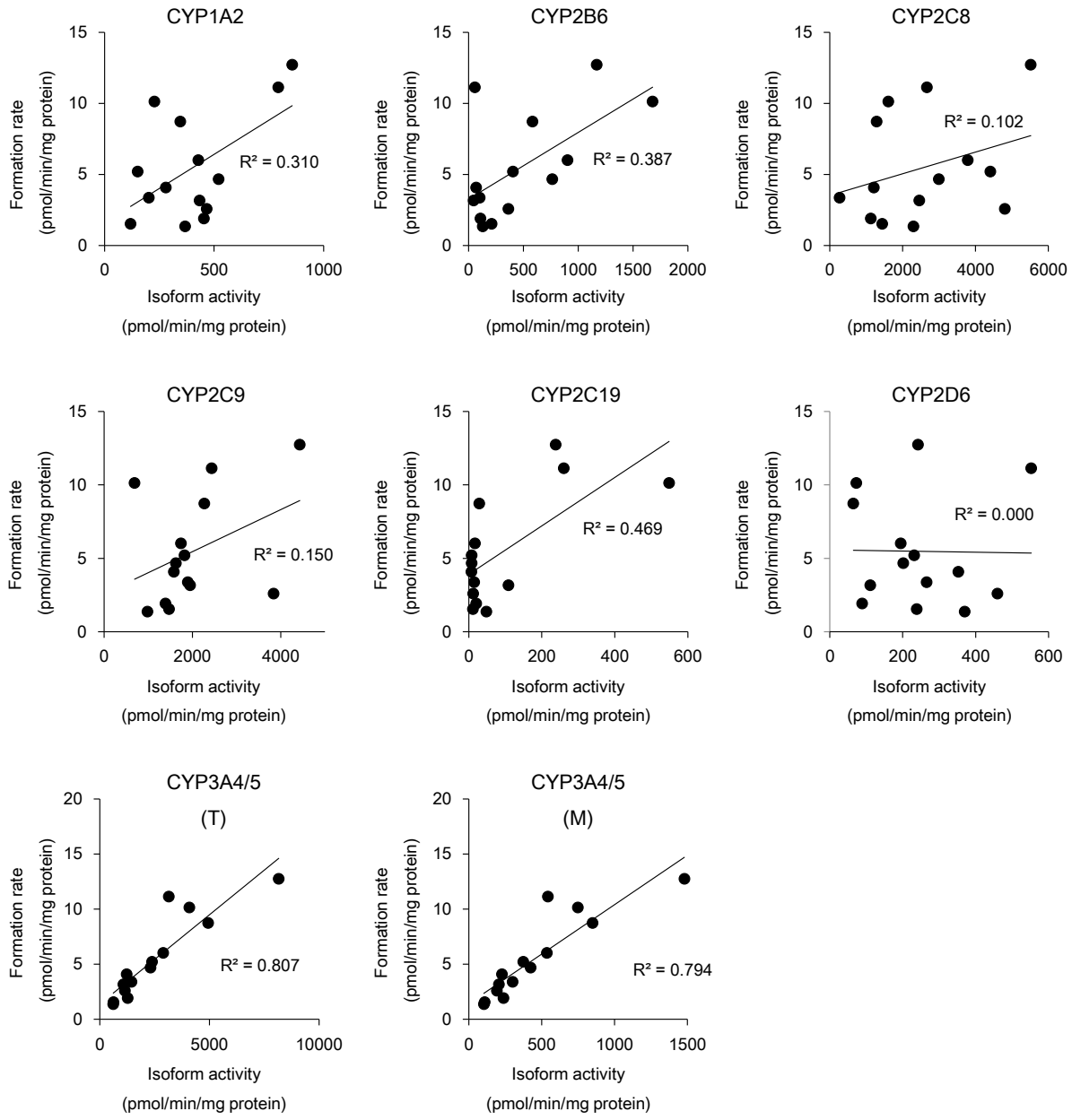
CYP1A2
Formation rate (pmol/min/mg protein)
R² = 0.310
Isoform activity (pmol/min/mg protein)
CYP2B6
R² = 0.387
CYP2C8
R² = 0.102
CYP2C9
R² = 0.150
CYP2C19
R² = 0.469
CYP2D6
R² = 0.000
CYP3A4/5 (T)
R² = 0.807
CYP3A4/5 (M)
R² = 0.794

**Supplemental Figure 3** Radioactivity concentrations in blood and plasma (A), cumulative excretion of radioactivity in urine and feces (B), and metabolite profiles in rat plasma (C) after single intravenous administration of [$^{14}$C]4MSA to male rat at 1 mg/kg.

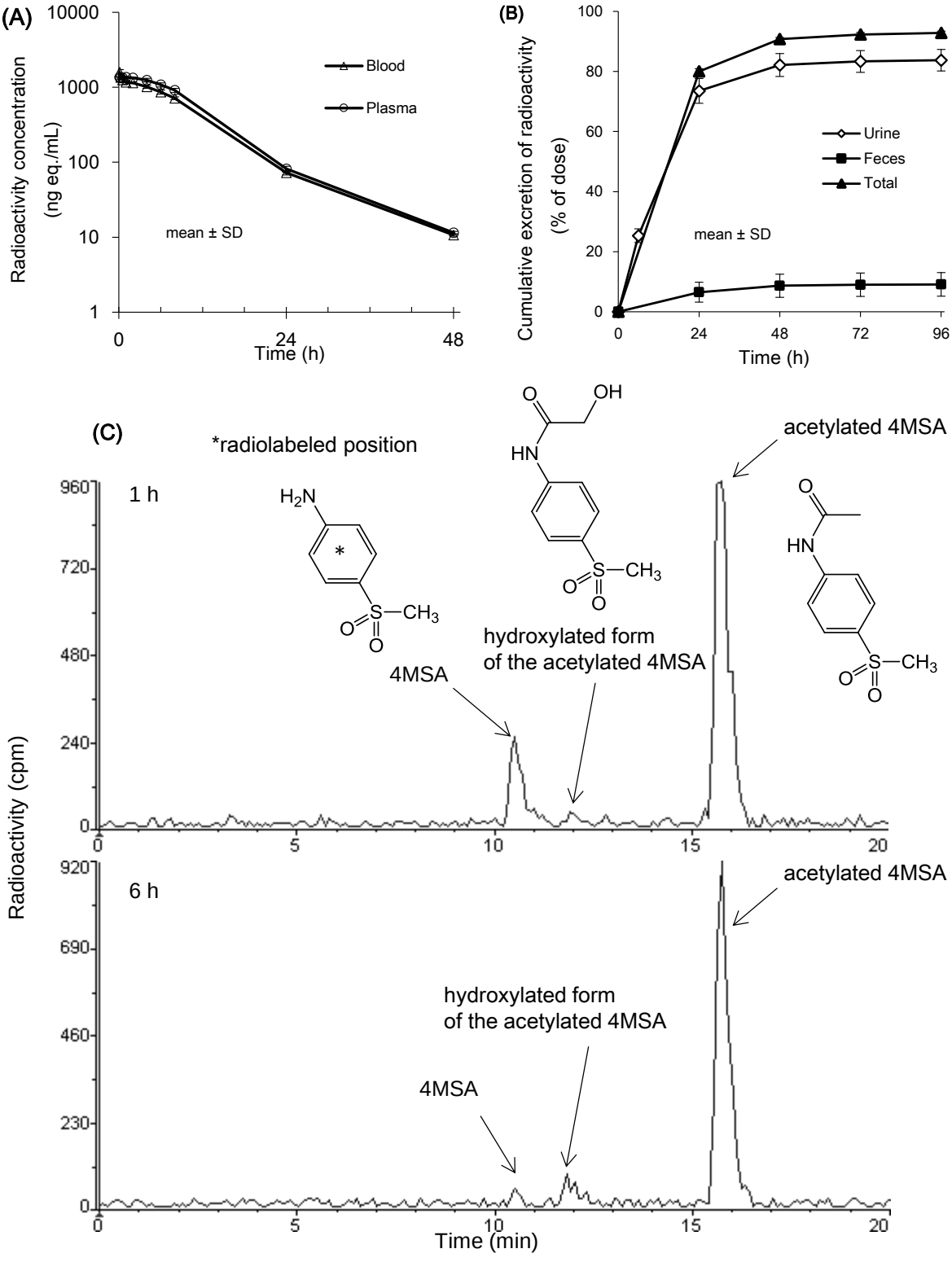

<Analytical Conditions of [$^{14}$C]4MSA >

Radio-HPLC analysis

Radio-HPLC analysis was conducted under the conditions described below.

· Apparatus for HPLC: ACQUITY UPLC PDA system (Waters Corp.)

· Radioactivity detector: Radiomatic 625TR (PerkinElmer, Inc.)

· Column: Inertsil ODS-3 (4.6 mm × 150 mm, 5 μm, GL Sciences Inc.)

· Column temperature: 50°C

· Detection: Radioactivity ($^{14}$C), UV (210 to 400 nm)

· Flow-rate of mobile phase for HPLC: 1 mL/min

· Mobile phase for HPLC: A, water containing 0.1% (v/v) formic acid; B, acetonitrile containing 0.1% (v/v) formic acid

· Gradient elution program: B(%) 5 (0 to 5 min) – 15 (15 min) – 70 (18 to 20 min)

· Sample cooler temperature: 8°C

· Liquid scintillator for radioactivity detection: Ultima-Flo M (PerkinElmer, Inc.)

· Flow-rate of liquid scintillator for radioactivity detection: 3 mL/min, mixed with the eluate from HPLC

LC-MS and LC-MS/MS analysis

The HPLC analytical condition was the same as the radio-HPLC analysis. MS and MS/MS analysis were performed on an LTQ-Orbitrap XL (Thermo Fisher Scientific Inc.) coupled with the above HPLC system.

· Ionization mode: electrospray

· Polarity: positive ion

· Electrospray voltage: 4.2 kV

- Capillary temperature: 275°C
- Sheath gas flow-rate: 30 arbitrary units
- Auxiliary gas flow-rate: 15 arbitrary units
- Activation type (MS/MS): HCD
- Isolated ion width (MS/MS): 4 *m/z*
- Collision energy (MS/MS): 30%
- MS to Radio (or Waste) ratio: approximately 1:3